行政院國家科學委員會專題研究計畫　期中進度報告

含有多立面倍半矽氧烷寡聚體或樹枝狀側鏈之發光高分子之合成與研究(1/2)

計畫類別：個別型計畫
計畫編號：NSC94-2216-E-009-017-
執行期間：94 年 08 月 01 日至 95 年 07 月 31 日
執行單位：國立交通大學材料科學與工程學系(所)

計畫主持人：韋光華

計畫參與人員：周嘉宏、許碩麟、張耀德

報告類型：精簡報告

處理方式：本計畫可公開查詢

中　華　民　國 95 年 5 月 22 日

行政院國家科學委員會補助專題研究計畫 ☑ 成 果 報 告 □期中進度報告

含有多立面倍半矽氧烷寡聚體或樹枝狀側鏈之發光高分子之合成與研究(I)(II)

計畫類別：☑ 個別型計畫　　□ 整合型計畫
計畫編號：NSC 94－2216－E－009－017－
執行期間：　94 年　8 月　1 日至　　95 年 7 月 31 日

計畫主持人：韋光華
共同主持人：
計畫參與人員： 周嘉宏　許碩麟　張耀德

成果報告類型(依經費核定清單規定繳交)：□精簡報告　☑完整報告

本成果報告包括以下應繳交之附件：
□赴國外出差或研習心得報告一份
□赴大陸地區出差或研習心得報告一份
□出席國際學術會議心得報告及發表之論文各一份
□國際合作研究計畫國外研究報告書一份

處理方式：除產學合作研究計畫、提升產業技術及人才培育研究計畫、列管計畫及下列情形者外，得立即公開查詢
□涉及專利或其他智慧財產權，□一年□二年後可公開查詢

執行單位：

中　華　民　國　95 年　　5　　月　　15　日

含有多立面倍半矽氧烷寡聚體或樹枝狀側鏈之發光高分子之合成與研究(I)(II)

研究計畫中英文摘要

中文摘要:

本案之分子設計藉由引入(1)高立體障礙結構及高熱穩定性之 POSS 孔洞材料及(2)樹枝狀側鏈，避免分子間堆疊所導致的自我驟息現象。利用不同功能的共軛基團引入，可開發不同需求藍色發光材料或紅光系材料。不但可有效地提昇螢光及電激發光效率至原來之兩倍至三倍，同時也增強原本材料在製程元件後的穩定度及電性。

關鍵字: 多立面倍半矽氧烷寡聚體; 發光高分子; 高分子發光二極體

Synthesis and Characterization of Luminescent Polyphenyl vinylene Incorporating Side-Chain-Tethered Polyhedral Oligomeric Silsesquioxane or dendritic structure Units

英文摘要:

We have synthesized, using the Gilch polymerization method, a new series of high-brightness, soluble copolymers (POSS-PPV-*co*-MEHPPV) of poly(*p*-phenylenevinylene) (PPV) containing side-chain-tethered polyhedral oligomeric silsesquioxane (POSS) pendent units and poly(2-methoxy-5-[2-ethylhexyloxy]-1,4-phenylenevinylene) (MEHPPV). This particular molecular architecture of POSS-PPV-*co*-MEHPPV copolymers possesses not only a larger quantum yield (0.85 vs. 0.19) but also higher degradation and glass transition temperatures relative to those of pure MEHPPV. The maximum brightness of a double-layered-configured light emitting diode (ITO/PEDOT/emissive polymer/Ca/Al) incorporating a copolymer of MEHPPV and 10 mol% PPV-POSS was five times as large as that of a similar light emitting diode incorporating pure MEHPPV (2196 vs. 473 cd/m^2). Moreover, we have also synthesized a thermally stable and high molecular weight fluorescent poly-(phenylenevinylene) (PPV) incorporating side-chain-tethered dendritic phenyl groups (DENPPV) through Gilch route; this DENPPV has a low abundance of tolane-bisbenzyl defects. Intramolecular energy transfer from the dendritic phenyl side group to the PPV backbone was evidenced from UV-vis and photoluminescence spectra of the DENPPV polymer and its model compound. Copolymers of DENPPV with 2-methoxy-5-(2-ethylhexyloxy) -1,4-phenylenevinylene (MEHPPV) display excellent photoluminescence both in solution and in the solid state; the highest quantum yield we observed was 82%. The electroluminescence of the copolymer MEHPPV/DENPPV (molar ratio: 25/75) was 70% higher than that of MEHPPV (0.12 lm/W vs. 0.07).

Keywords: POSS, Light-Emitting Polymer, PLED

計畫名稱: 含有多立面倍半矽氧烷寡聚體(POSS)於側鏈之發光高分子之合成與研究

第一章　研究計畫內容

1. 研究計畫之背景及目的

1-1. 多面體倍半矽氧烷寡聚物(POSS):

多面體倍半矽氧烷寡聚物/高分子奈米複合材料屬於金屬氧化物分子簇/高分子奈米複合材料的一種，自從 1993 年加拿大Air Force Research 實驗室將多面體倍半矽氧烷寡聚物(polyhedral oligomeric silsesquioxane (POSS))引入高分子中獲得突出之性質後，該倍半矽氧烷寡聚物受到多方的注意，並且由Hybrid Plastics公司將其量產，最早是在以溶膠-凝膠(sol-gel)法合成多孔性材料(zeolites)時被發現的【1】，多面體倍半矽氧烷寡聚物的化學結構是介於二氧化矽(SiO_2)和矽氧烷(R_2-SiO)之間，其化學結構式通常以$(RSiO1.5)_n$表示，圖一為其立體結構圖。多面體倍半矽氧烷寡聚物為單一分子結晶體、結構相當對稱、分子大小約為 0.7 nm 至 2 nm之間且對許多有機溶劑有良好的溶解度，是一種很適合用來製備有機-無機奈米複合材料的無機金屬氧化物寡聚物。其中以$(RSiO1.5)_8$這一系列多面體倍半矽氧烷寡聚物最常被用來與高分子結合刑成多面體倍半矽氧烷寡聚物/高分子奈米複合材料(POSS/polymer nanocomposites)。(以下將稱$(RSiO1.5)_8$這一系列多面體倍半矽氧烷寡聚物為POSS。)

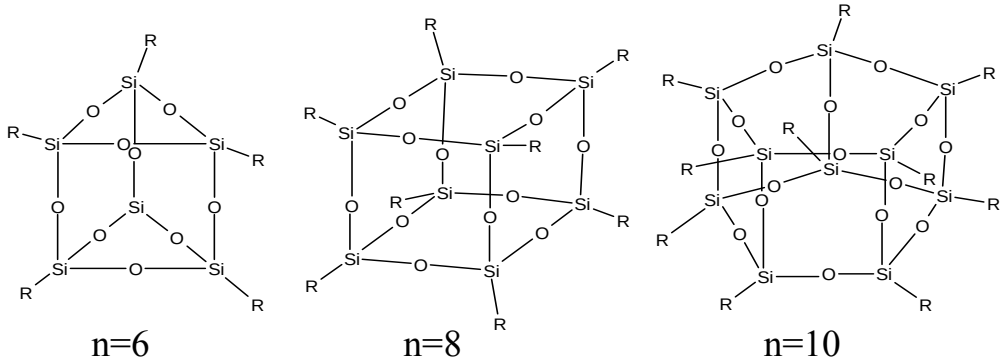

圖一. 多面體倍半矽氧烷寡聚物$(RSiO1.5)_n$的立體結構圖

圖二為 POSS 的化學立體結構圖，POSS 為一大小約為 1.5 nm 的六面體結晶體 (rhombohedral crystal structure) 【2】，其由一結構剛硬的六面體二氧化矽為中心及 8 個有機取代基接在矽上所組成。其結構上的有機取代基可分為兩大類，一為沒有反應性的有機取代基，可以增加 POSS 的溶解度及與高分子的相容性；一為單一或多個具反應性取代基，可與高分子刑成共價鍵連結。

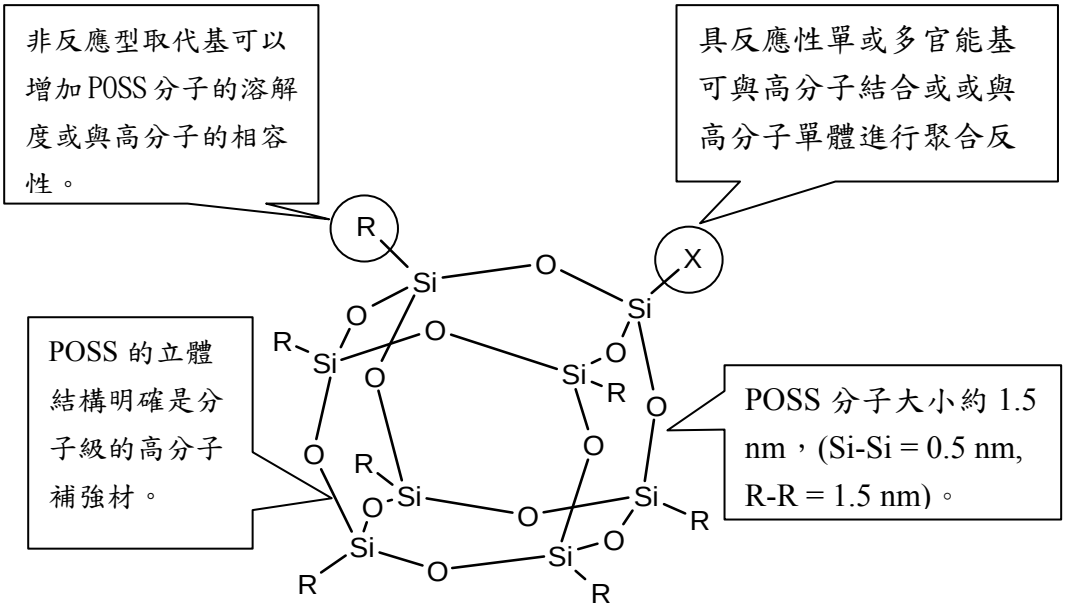

圖二. 多面體倍半矽氧烷寡聚物$(RSiO1.5)_8$ (POSS)的立體結構圖

反應式一為 POSS 的合成方法，反應式二為最常用來合成具不同官能基 POSS 的方法(如圖三)。

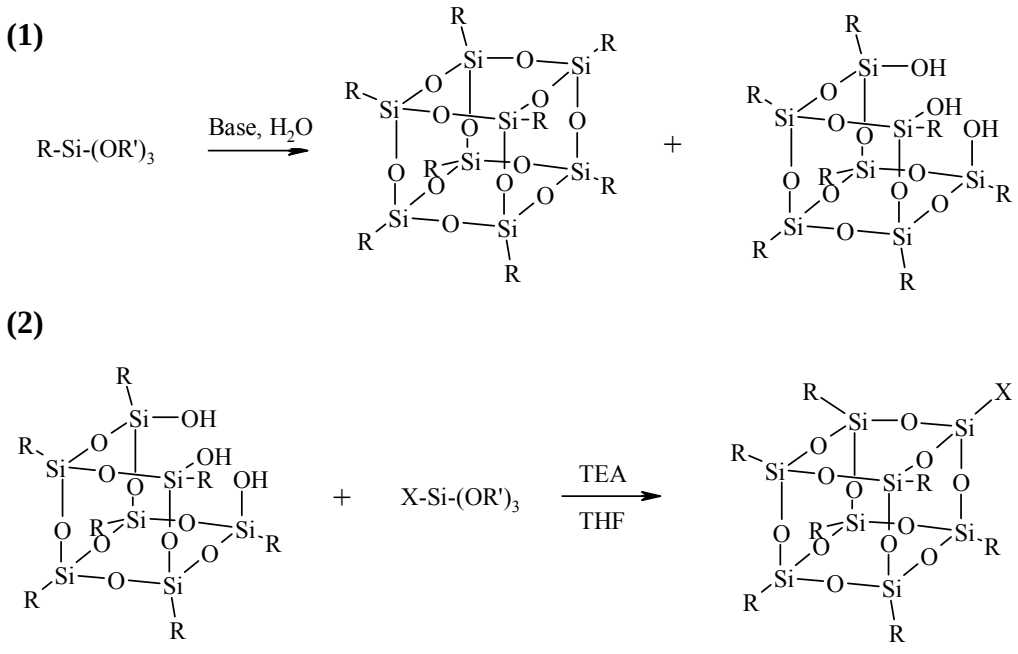

圖三. POSS 的合成方法及官能基改質方法

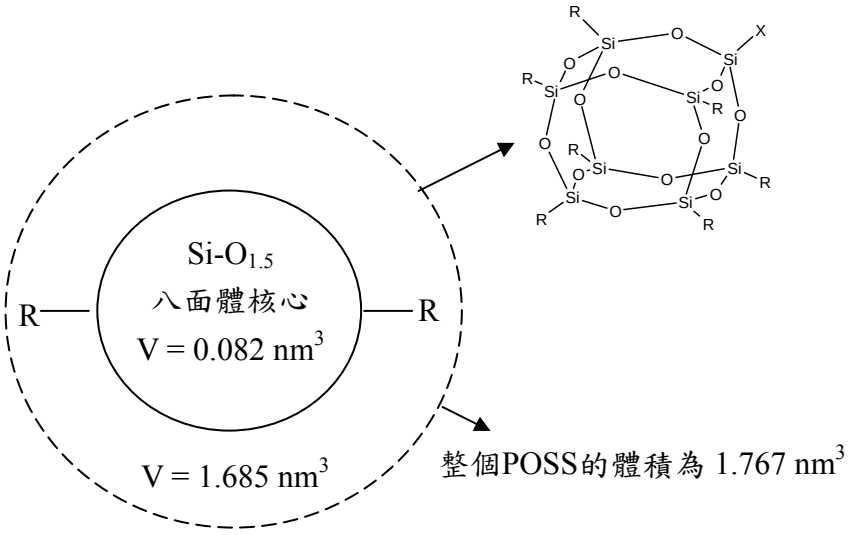

圖四. POSS 的結構與體積關係圖

另外，POSS 為一微孔性材料(micoporous materials)，其孔洞是存在於其結構中的六面體二氧化矽，孔洞大小約為 0.3-0.4nm【1】，(圖四) 。由於 POSS 分子為奈米級顆粒,並且與高分子之間相容性甚好，可以均勻地分散於高分子材料中，形成奈米級複合材料，達到良好補強效果。

1-2. POSS/高分子奈米複合材料的發展:

POSS分子自 1993 年來，以不同方式被引入高分子中來補強其熱性質及機械性質，其中具單反應官能基的POSS ($R_7R'Si_8O_{12}$)已經以單體的方式引入線性高分子中，其包括methacrylates【3】、styrenics【4,10】、norbornenes【5-6】和urethanes【7】等。另外，具多反應官能基的POSS分子以分子起始劑或交聯劑形成星狀或網狀結構高分子奈米複合材料【8-9】【11-12】。

POSS 分子除了加入高分子中當補強材外，另外可以用來合成其它功能性材料，如催化材料、孔洞性材料、發光材料與透氣膜材料。如此適用多功能應用乃因為 POSS 分子的高表面積、可控制的結構及多變化的官能基。雖然 POSS/高分子奈米複合材料的應用性受到大家注意但所有研究仍在初步研究階段，仍需更多及更深入研究來發研究及開發更多的 POSS/高分子奈米複合材料。

1-3. POSS/高分子光電複合材料

相較於無機半導體發光二極體需要高真空、高溫之製程環境，高分子發光二極體具有製程簡便、易大面積化及可製作撓曲形狀元件的優勢，亦是工業上極具發展潛力的材料。多立面倍半矽氧烷寡聚體(POSS) 本身屬多孔洞無機材料，耐熱性及熱穩定性優異，導入高分子(如:聚亞醯胺(PI))中可降低材料本身的介電係數(dielectric constant)，大幅提升材料的應用價值。本實驗室已合成出一系列之 PF-POSS 高分子(如圖五、圖六)，已發表並將刊登於 Macromolecules 期刊【13】。

除此之外，近期來已有探討 POSS 與應用於光電材料的文獻，主要可分為三類:

1. 將 POSS 官能基鍵結於高分子尾端(end-capped) 【14】: 將 POSS 鍵結於 PF(polyfluorene) 及 MEHPPV 的尾端，提高元件整體的光電性質。
2. 星狀結構(Star-like)之 poss【15】: 以 POSS 為中心，與 PF(polyfluorene)結合成星狀結構(Star-like)。可提高材料的熱穩定度、元件的光電性質、EL 光色純度。
3. 側鏈(side chain) 鍵結 POSS 結構: 相較於其他兩種方式 POSS 於高分子中的含量(Starlike 3.8%， end-capped 1.2%)，側鏈(side chain) 鍵結 POSS 的方法提供了較大的變化性。由於其鍵結端位於高分子側鏈，一方面可藉由合成含 POSS 之單體與其他單體聚合，藉以控制 POSS 在高分子中的含量，可測試出最有效的比例; 另外由於導入此巨大官能基於側鏈上，也可以防止高分子堆疊(aggregation)所造成的自我驟息(self-quench)，提高元件整體的發光效益。

我們在設計整個分子結構將考量合成簡易性即可溶性，第一年將藉由化學合成法嘗試導入 POSS 於一般常見高量子效率之發光高分子，如 Polyfluorene, polyphenylvinylene……dendritic 等，製程元件並量測其光電性質。第二年計畫將著重於 polymer 的改質(合成樹枝狀 PPV)、元件製程的改良與 morphology 的研究。

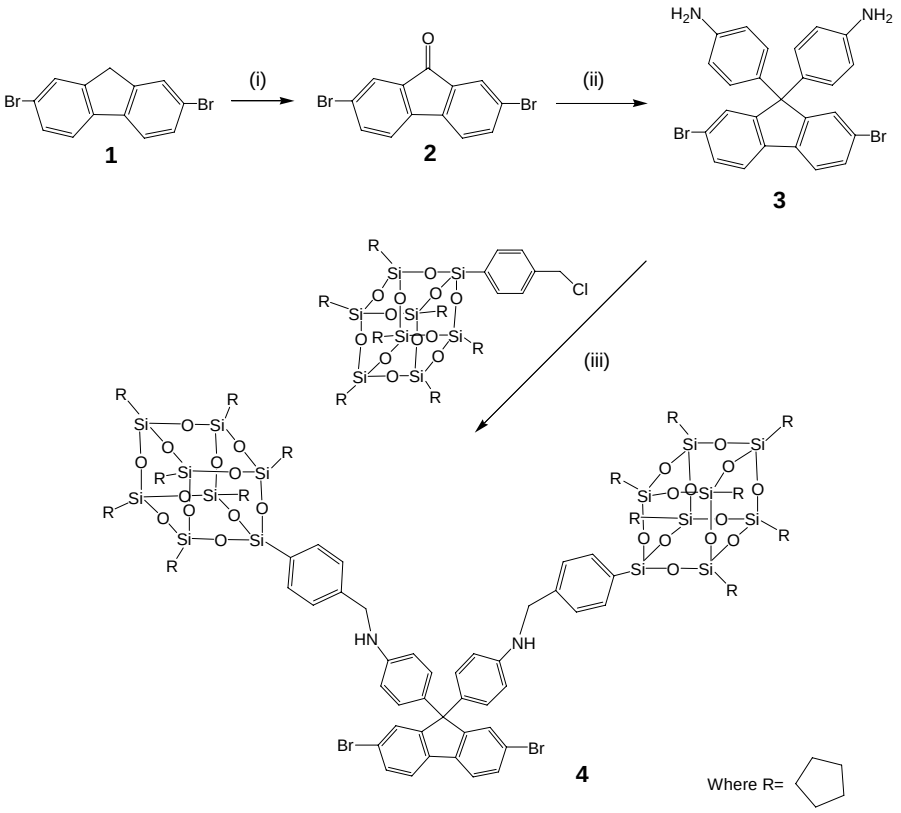

圖五. 本實驗室合成出之 POSS 單體

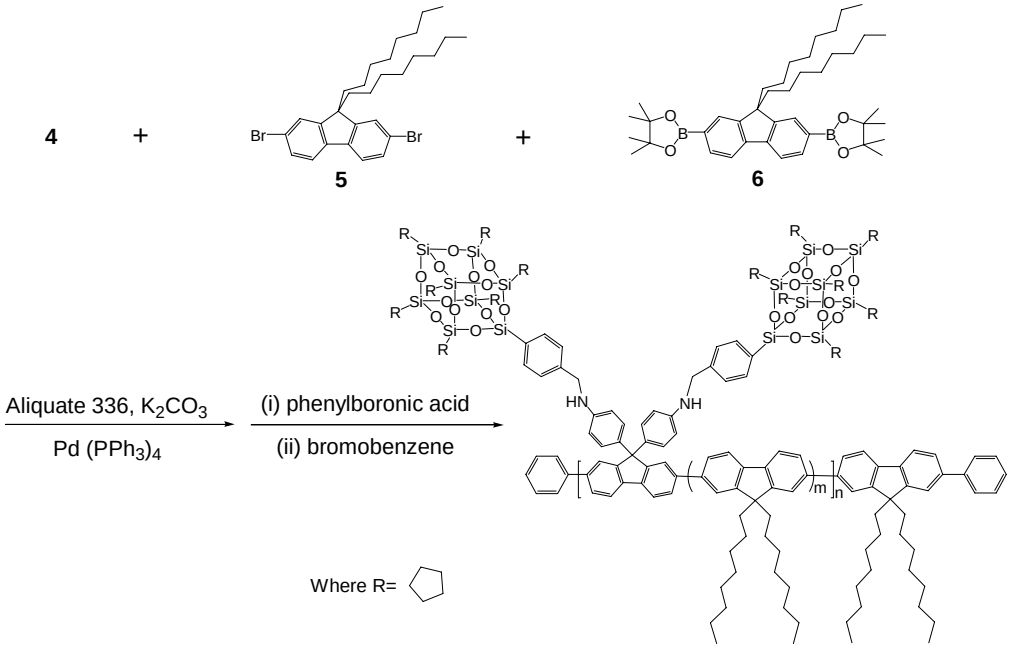

圖六. 本實驗室合成出之 PFO-POSS copolymer

1-4. 結果與討論:

首先我們先合成含有 POSS 的側鏈分子，利用 Gilch 途徑共聚合時趨向於形成交替型共聚物。而其合成方法如下(b)：

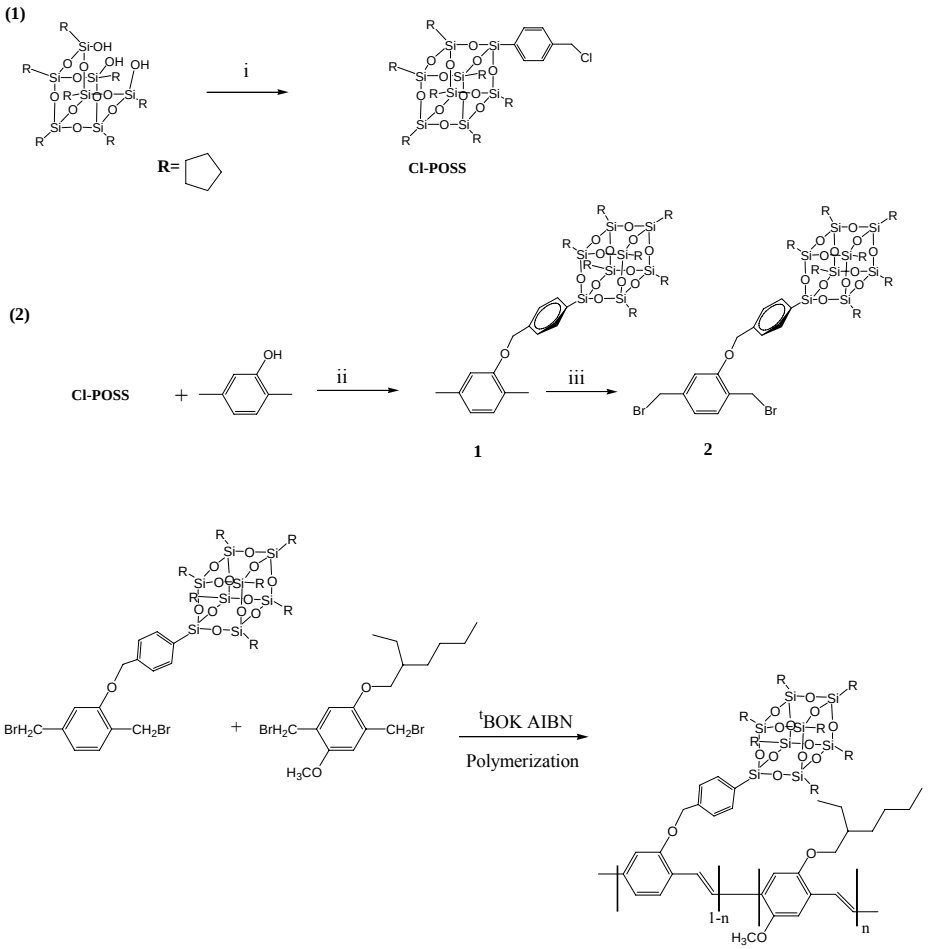

製程出以多立面倍半矽氧烷寡聚體(POSS)/Conducting polymer 奈米複合材料為發光層之 LED 元件。初期希望可控制半導體奈米量子點的 particle size 與表面官能基的置換，並將合成出之高分子完成物性、結構鑑定與基本光學性質的量測。接下來已完成 POSS/ 高分子奈米複材的製作與製程條件的測試，在製作的過程中尋找改進的方法，進一步探討不同濃度配比與 particle size 對物理及光學性質的影響，最後以適當比例條件製成元件後，量測量子效率及 EL 元件性質；預期與同類元件相比，能明顯提高其發光效率。

Table 1. Optical Properties of the **POSS-PPV-*co*-MEHPPV** Nanocomposites.

	λ_{max} (UV, nm)		λ_{max} (PL, nm)[a]		Q.Y
	solution[b]	film	solution[b]	film	film[c]
MEHPPV	499	517	553 (592)	591 (634)	0.19
POSS-PPV1-*co*-MEHPPV	499	512	552 (591)	588 (633)	0.43
POSS-PPV3-*co*-MEHPPV	498	512	552 (591)	586 (632)	0.62
POSS-PPV5-*co*-MEHPPV	497	511	552 (591)	585 (631)	0.84
POSS-PPV10-*co*-MEHPPV	494	505	551 (590)	584 (631)	0.87

[a] The data in parentheses are the wavelengths of the shoulders and subpeaks.

[b] The absorption and emission were measured in THF.

[c] PL quantum yield estimated relative to a sample of Rhodamine 6G (Φ_{FL} = 0.95).

在量子產率的測量上，亦是利用已知在 Rhodamine 6G 作為標準品，**POSS-PPV10-*co*-MEHPPV** 結構最高可達 0.87。此外放射半波高寬也相當的窄（小於 100 nm），這對光色上的純度有很佳的助益。

電性方面的特性，對於製程雙層結構之LED元件(ITO/PEDOT:PSS/polymer /Ca/Al)，分析如下:

1. 固態PL (圖一): 導入POSS 的 PPV高分子，熱性質明顯提升。
2. 元件EL (圖二): 原材料MEHPPV 之EL 放光 為橘紅光 (590 nm) ，經由導入POSS後，半高寬(FWHM)明顯驟減，自110 nm降低至75 nm(抑制excimer生成)，提高原本光色純度。
3. I-V and L-V curve(圖三及圖四): 導入POSS 的 PPV高分子，元件可乘載的電流值明顯提升，因此在亮度部分增強為原來的四倍(2196 vs. 473 cd/m^2)。

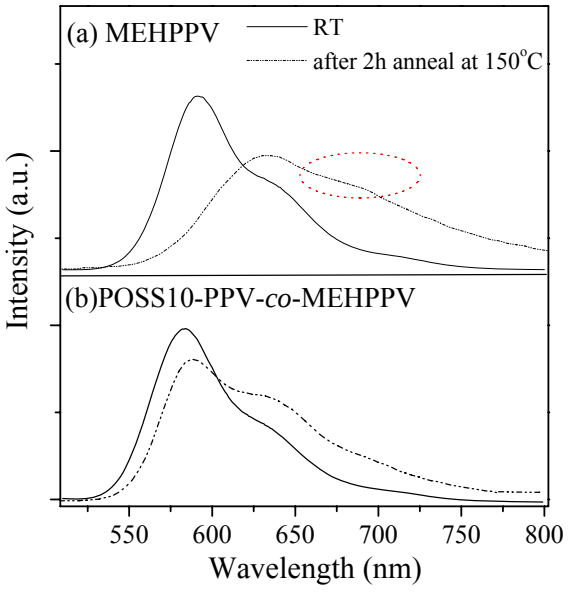

(圖一)

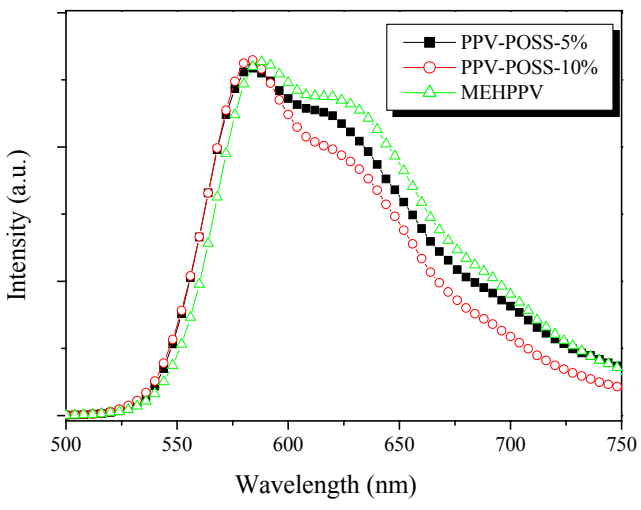

(圖二)

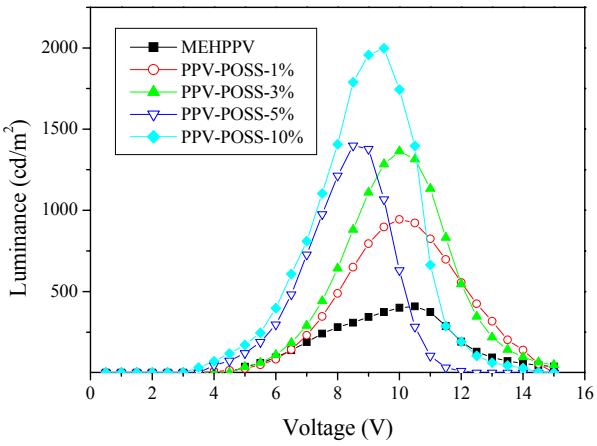

(圖三)

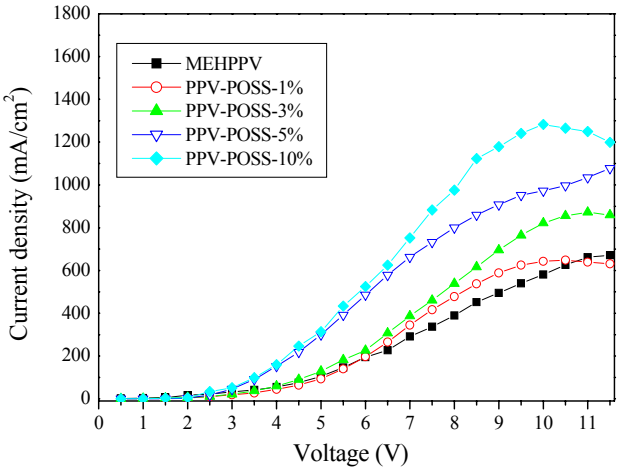

(圖四)

對現有的平面顯示器而言，在大尺寸領域裡，因電漿激發顯示技術的發展，促使電漿顯示器在商品化上大步邁進，但在製作良率和價格上仍然有待克服。在中小尺寸中，最成熟且廣泛應用的是液晶顯示器，但產品受限於畫質、應答速度和對溫度的穩定性。對於有機電激發光顯示技術而言，小分子系統在中小尺寸較占優勢，已有許多商業化產品，高分子系統雖然進展較慢，商業化產品較少，然而一旦在材料與噴墨列印量產技術上有所突破，必能在大尺寸與可撓曲的顯示器上大放異彩。本計畫之特色在於導入 POSS 於高分子材料，以提高此種奈米複合材料製成之發光二極體元件的電激發光效率。由於使用同一種材料製作，製程較容易，運用此改質方法結合之高分子奈米複合材料，可得到一均勻密度的薄膜，提高發光高分子之發光效率、元件效率並提升其耐熱度及使用壽命。

2.參考文獻:

1. C. Zhang, F. Babonneau, C. Bonhomme, R. M. Laine, C. L. Soles, H. A. Hristov, A. F. Yee, *J. Am. Chem. Soc.* **1998**, *12*0, 8380.
2. L. Zheng, A. J. Waddon, R. J. Farris, E. B. Coughlin, *Macromolecules* **2002,** *35,* 2375.
3. F.Gao, B. M. Culbertson, Y. Tong, S. R. Schricker, *Polym. Prepr.* **2001**, *41*, 580.
4. A. Romo-Uribe, P. T. Mather, T. S. Haddad, J. D. Lichtenhan, *J. Polym. Sci., Part B: Polym. Phys.* **1998**, *36*, 1857.
5. P. T.Mather, H. G. Jeon, A. Romo-Uribe, T. S. Haddad, J. D. Lichtenhan, *Macromolecules* **1999**, *32*, 1194.
6. R. K. Bharadwaj, R. J. Berry, B. L. Farmer, *Polymer* **2000**, *41*, 7209.
7. B. X. Fu, B. S. Hsiao, H. White, M. Rafailovich, P. T. Mather, H. G. Jeon, S. Phillips, J. D. Lichtenhan, J. J. Schwab, *Polym. Int.* **2000**, *49*,437.
8. J. Choi, J. Harcup, A. F. Yee, Q. Zhu, R. M. Laine, *J. Am. Chem. Soc.* **2001**, *123*, 11420.
9. R. Tamaki, Y. Tanaka, M. Z. Asuncion, J. Choi, R. M. Laine, *J. Am. Chem. Soc.* **2001**, *123*, 12416.
10. T. S. Haddad, J. D. Lichtenhan, *Macromolecules* **1996**, *29*, 7302.
11. C. Zhang, R. M. Laine, *J. Am. Chem. Soc.* **2000** *122*, 6979.
12. R. M. Laine, J. Choi, I. Lee, *Adv. Mater.* **2001**, *1*3, 800.
13. Chou, C. H.; Hsu, S. L.; Dinakaran, K. ; Chiu, M. Y.; Wei, K. H. *Macromolecules* **2004**, accepted.
14. Xiao, S.; Nguyen, M.; Gong, X.; Cao, Y.; Wu, H.; Moses, D.; Heeger, A. J. *Adv. Funct. Mater.* **2003**, *13*, 25.
15. Lin, W. J.; Chen, W. C.; Wu, W. C.; Niu, Y. H.; Jen, A. K. Y. *Macromolecules* **2004**, *37*, 2335.

3. 計畫成果自評

3-1.第一年度預期工作項目及進度：

年度	94 年度						94～95 年度					
季別	第 一 季			第 二 季			第 三 季			第 四 季		
工作項目	七月	八月	九月	十月	十一月	十二月	一月	二月	三月	四月	五月	六月
參考資料之蒐集與研讀、化學藥品之購得、儀器與製作流程之熟悉	→											
多立面倍半矽氧烷寡聚體(POSS) 之合成		→	→									
高分子單體的合成			→	→	→							
高分子材料的合成、分子量的控制與結構的鑑定					→	→						
量測不同濃度配比對物理及光學性質的影響(熱性質研究)						→	→	→				
量測固態薄膜光學性質/改變參數並製成元件比較								→	→	→		
量子效率及 EL 元件性質之量測										→	→	
報告之撰寫												→
預定累積進度	30 %			50 %			80 %			100 %		

3-2. 預期進度之完成與檢討:

已完成預期今年度之實驗內容並進行至第二年度的工作，部分研究工作內容已撰寫成學術論文投稿，經過審查並發表於 ACS 之期刊中。

共分為兩部分:

1. Kannaiyan Dinakaran, Shu-Min Hsiao, Chia-Hung Chou, So-Lin Shu and Kung-Hwa Wei* “Synthesis and characterization of an efficiently fluorescent polyphenylenevinylene possessing pendant dendritic phenyl groups” *Macromolecules* **2005**, *38*(25), 10429.
2. Chia-Hung Chou, So-Lin Hsu, Siao-Wei Yeh, Hsu-Shen Wang, Kung-Hwa Wei “Enhanced Luminance and Thermal Properties of Polyphenylenevinylene Copolymer Presenting Side-Chain-Tethered Silsesquioxane Units” *Macromolecules* **2005**, *38*(22), 9117.

研究中，製程出以多立面倍半矽氧烷寡聚體(POSS)/Conducting polymer 奈米複合材料為發光層之 LED 元件。初期希望可控制半導體奈米量子點的 particle size 與表面官能基的置換，並將合成出之高分子完成物性、結構鑑定與基本光學性質的量測。接下來希望能完成 POSS/高分子奈米複材的製作與製程條件的測試，在製作的過程中尋找改進的方法，再進一步探討不同濃度配比與 particle size 對物理及光學性質的影響，最後以適當比例條件製成元件後，量測量子效率及 EL 元件性質。

3-3. 下一年度計畫執行:

由於本計劃屬有機無機之高分子奈米複合材料之光電性質探討，整體來說，對於參與研究生之訓練較具多元性，其中囊括:複合材料結構設計、有機無機材料製備合成技術、化學結構鑑定、材料性質量測鑑定(表面微結構、熱性質及光電性質)、元件製程及量測技術……等。導入無機材之技術若能充分利用，即可應用在多種類之高分子發光材料上;如此一來，不僅保有高分子容易大面積化、製程容易、成本較低等優點，結合易製備、光電特性佳的奈米複材，除了對於 PLED 往後在材料選擇及結構設計上，有許多可以發展空間外; 也期望研究能實際應用於產業界，在未來能結合現有之顯示技術而達到全彩化及大面積、高品質、低成本的顯示器，提高國內顯示科技研發之技術。在明年的計畫部分，期望能進一步利用化學鍵結合奈米粒子於高分子中並提升高分子之光電性質。

可供推廣之研發成果資料表

□ 可申請專利　□ 可技術移轉　日期：95 年 5 月 15 日

國科會補助計畫	計畫名稱： 含有多立面倍半矽氧烷寡聚體或樹枝狀側鏈之發光高分子之合成與研究 計畫主持人：韋光華 計畫編號： NSC 94－2216－E－009－017－ 學門領域： 工程處
技術/創作名稱	側鏈含有多立面倍半矽氧烷寡聚體之發光高分子材料
發明人/創作人	韋光華
技術說明	**中文：**大部份的電激發光高分子，由於天生有著豐富的π電子，因此電洞注入特性和傳輸電洞的能力遠比電子注入特性和傳輸電子的能力來的有效率。因此，為了增加元件的效率，合成高效率的電子傳輸高分子是必要的。聚奎林高分子（Polyquinoline）及其衍生物是最近發表可以應用在二極體上的電子傳輸層的高分子，因為它們有高熱穩定性、高抗氧化能力、優異的機械性質和良好的成膜能力。然而，卻有一個缺點---溶解度不好。　　氟（Fluorene）的衍生物由於包含一剛性且共平面的雙苯環結構，所以表現出特殊的物理和化學性質，再加上在氟上 C9 的位置接上不同的取代基可以增加溶解度且不會明顯的增加高分子骨幹間的立體作用力。且氟的高量子效率和優良的熱穩定度，與氟共聚合的高分子變成了最吸引人的藍光發光材料。然而，無論是 PPV 或者是 PF 系列元件在製成薄膜時，由於材料累積濃度過高造成分子堆疊，甚至於產生 excimer，嚴重影響了光色以及降低了發光效率;此外，PF 系列由於 C9 位置容易產生氧化現象(keto defect)，也會改變元件原有的發光光色。 為了改善這些缺點，選擇導入 POSS 於高分子材料期望以考量製程簡單與成本低廉的條件之下能對於高分子的性質做一些改良，並利用無機材的良好耐熱特性與分子結合，使之可以更加廣泛的應用在顯示器的發光材料上。此方法所合成之高分子奈米複合材料可提高發光高分子之發光效率、元件效率並提升其耐熱度及使用壽命。

	英文：We have synthesized, using the Gilch polymerization method, a new series of high-brightness, soluble copolymers (POSS-PPV-*co*-MEHPPV) of poly(*p*-phenylenevinylene) (PPV) containing side-chain-tethered polyhedral oligomeric silsesquioxane (POSS) pendent units and poly(2-methoxy-5-[2-ethylhexyloxy]-1,4-phenylenevinylene) (MEHPPV). This particular molecular architecture of POSS-PPV-*co*-MEHPPV copolymers possesses not only a larger quantum yield (0.85 vs. 0.19) but also higher degradation and glass transition temperatures relative to those of pure MEHPPV. The maximum brightness of a double-layered-configured light emitting diode (ITO/PEDOT/emissive polymer/Ca/Al) incorporating a copolymer of MEHPPV and 10 mol% PPV-POSS was five times as large as that of a similar light emitting diode incorporating pure MEHPPV (2196 vs. 473 cd/m^2).
可利用之產業 及 可開發之產品	1. 光電產業; OLED/PLED 相關。 2. 產率高，步驟簡單的優勢。在元件效能表現上，發光效率可達 0.87，光電效率也隨之提升。全新核心結構，可依此無限延伸，開發其他新型有機半導體材料及其應用產品; 如此一來，不僅保有高分子容易大面積化、製程容易、成本較低等優點，結合易製備、光電特性佳的奈米複材，除了對於 PLED 往後在材料選擇及結構設計上，有許多可以發展空間外; 也期望研究能實際應用於產業界，在未來能結合現有之顯示技術而達到全彩化及大面積、高品質、低成本的顯示器，提高國內顯示科技研發之技術。
技術特點	本案之技術中心在於結合高熱穩定性之 POSS 與發光高分子，提高此種奈米複合材料製成之發光二極體元件的電激發光效率。藉由改變 POSS 導入的單體濃度，可控制不同的成分比; 由於使用同一種材料製作，製程較容易，運用此方法結合之奈米複合材料，可得到一均勻密度的有機薄膜，並提升原本 EL 之強度。
推廣及運用的價值	對現有的平面顯示器而言，在大尺寸領域裡，因電漿激發顯示技術的發展，促使電漿顯示器在商品化上大步邁進，但在製作良率和價格上仍然有待克服。在中小尺寸中，最成熟且廣泛應用的是液晶顯示器，但產品受限於畫質、應答速度和對溫度的穩定性。對於有機電激發光顯示技術而言，小分子系統在中小尺寸較占優勢，已有許多商業化產品，高分子系統雖然進展較慢，商業化產品較少，然而一旦在材料與噴墨列印量產技術上有所突破，必能在大尺寸與可撓曲的顯示器上大放異彩。本申請案之特色在於導入POSS於高

	分子材料，以提高此種奈米複合材料製成之發光二極體元件的電激發光效率。由於使用同一種材料製作，製程較容易，運用此改質方法結合之高分子奈米複合材料，可得到一均勻密度的薄膜，提高發光高分子之發光效率、元件效率並提升其耐熱度及使用壽命。

※ 1.每項研發成果請填寫一式二份，一份隨成果報告送繳本會，一份送貴單位研發成果推廣單位（如技術移轉中心）。

※ 2.本項研發成果若尚未申請專利，請勿揭露可申請專利之主要內容。

※ 3.本表若不敷使用，請自行影印使用。

附錄:

1. Kannaiyan Dinakaran, Shu-Min Hsiao, Chia-Hung Chou, So-Lin Shu and Kung-Hwa Wei* "Synthesis and characterization of an efficiently fluorescent polyphenylenevinylene possessing pendant dendritic phenyl groups" *Macromolecules* **2005**, *38*(25), 10429.

2. Chia-Hung Chou, So-Lin Hsu, Siao-Wei Yeh, Hsu-Shen Wang, Kung-Hwa Wei "Enhanced Luminance and Thermal Properties of Polyphenylenevinylene Copolymer Presenting Side-Chain-Tethered Silsesquioxane Units" *Macromolecules* **2005**, *38*(22), 9117.

Synthesis and Characterization of an Efficiently Fluorescent Poly(phenylenevinylene) Possessing Pendant Dendritic Phenyl Groups

K. Dinakaran, Shu-Min Hsiao, Chia-Hung Chou, So-Lin Shu, and Kung-Hwa Wei*

Department of Materials Science and Engineering, National Chiao Tung University, Hsinchu, Taiwan 30049, R.O.C.

Received February 4, 2005; Revised Manuscript Received August 10, 2005

ABSTRACT: We have synthesized a thermally stable and high molecular weight fluorescent poly(phenylenevinylene) (**PPV**) incorporating side-chain-tethered dendritic phenyl groups (**DENPPV**) through Gilch route; this **DENPPV** has a low abundance of tolane-bisbenzyl defects. Intramolecular energy transfer from the dendritic phenyl side group to the **PPV** backbone was evidenced from UV−vis and photoluminescence spectra of the **DENPPV** polymer and its model compound. Copolymers of **DENPPV** with 2-methoxy-5-(2-ethylhexyloxy)-1,4-phenylenevinylene (**MEHPPV**) display excellent photoluminescence both in solution and in the solid state; the highest quantum yield we observed was 82%. The electroluminescence of the copolymer **MEHPPV/DENPPV** (molar ratio: 25/75) was 70% higher than that of **MEHPPV** (0.12 lm/W vs 0.07).

Introduction

Electroluminescence devices based on organic thin films are of great interest because of their potential applications as large-area light-emitting displays that require a low driving voltage and have good processability and a fast response time.[1] Although many poly(phenylenevinylene) (**PPV**) derivatives have been synthesized and applied in light-emitting diode (LED) applications, very few display high photoluminescence efficiencies.[2] There are a number of reasons for these low photoluminescence efficiencies: (a) Conjugated backbones tend to stack cofacially with one another as a result of favorable interchain π-π interactions, which leads to a self-quenching of excitons. (b) An imbalance of hole/electron injection and transport occurs in the emission layer in devices because most emissive polymers conduct holes in preference to electrons.[3] (c) Trapping of excitons by defect sites in the polymer backbone causes nonradiative decay. These structural defects in the polymer not only reduce the photoluminescence quantum yield but also are responsible for the short operational lifetimes of LED devices.[4]

Various techniques have been proposed to improve the efficiency of **PPV**s, either by modifying their chemical structure with bulky side groups or by using a copolymerization approach to incorporate conjugated phenylenevinylene segments among nonconjugated spacers.[5] For example, soluble **PPV** derivative with bulky alkoxy side groups, poly[2-methoxy-5-(2-ethylhexyloxy)-1,4-phenylenevinylene] (**MEHPPV**) has been developed.[6−9] More recently, various bulky substituents, such as alkoxy, alkylsilyl, phenyl, and fluorenyl groups, have been substituted at the 2- or 2,5-positions of the **PPV** backbone to suppress the aggregation, caused by intermolecular interactions, that quench the formation of excimers.[9,10] Three new soluble **PPV** derivatives have been obtained through use of the Horner−Witting−Emmons (HWE) reaction; these materials in the solid state display a photoluminescence quantum yields of 61%,[10d] which is higher than that of **MEHPPV**. One weak feature of **PPV** derivatives that have flexible side chains is that they are sensitive to a combination of air and light.[11] In contrast, phenyl-substituted **PPV**s have higher resistance to photooxidation than do other substituted **PPV**s.[12] LEDs having longer lifetimes can be fabricated from a single phenyl group substituted **PPV**s that contain few head-to-head (HH) and tail-to-tail (TT) couplings,[13,14] such couplings referred to as tolane−bis(benzyl) (TBB) defects. It has also been demonstrated that polymers presenting fourth-generation dendrimers have a diminished amount of intermolecular π-stacking and, consequently aggregate formation is inhibited.[15] The photonic effects observed by the dendronization of polymers have been explored in recent years.[16] We have already demonstrated that higher luminescence efficiencies exist for polyfluorenes possessing side-chain tethered polyhedral oligomeric silsesquioxane (POSS).[17a] Moreover, Frechet-type dendrimers, a benzyl alcohol dendrimer, have been shown to have high photoluminescence.[17b] In contrast to the Frechet-type dendrimers, Mullen-type dendrimers,[18,19] which are polyphenylene dendrimers, are both shape-persistent and chemically stable. Therefore, their π-stacking is precluded at lower dendritic generations than it is for the Frechet type. Their three-dimensional shielding ability has been demonstrated by using perylene dyes as core units.[18] The Mullen type dendrimers do not interfere with the charge transport or emission properties of the polyfluorene. Dendrimer substitution has been performed to hinder excimer formation and exciton migration to oxidized ketonic sites, which thereby increases the color stability of the devices.[19] In the present study, we have employed the dendritic phenyl (Mullen-type) **PPV**, which offers the following advantages: (i) It permits spatial control of the polymer chain and shields it from interchain excimer formation; (ii) it is a fully conjugated **PPV**; (iii) it provides a very low abundance of TBB defects as a result of electronic (the stronger acidity of the bromomethyl moiety at the ortho position of the highly conjugated dendritic phenyl group) and steric effect of the substituent; (iv) its rigid aromatic structure provides higher stability to thermal oxidation; (v) its excitation energy is transferred to the polymer

* Corresponding author. E-mail: khwei@cc.nctu.edu.tw. Telephone: 886-35-731871. Fax: 886-35-724727.

10.1021/ma050252q CCC: $30.25
Published on Web 11/12/2005

backbone, which leads to enhanced device performance and quantum efficiency. The preparation of this polymer is also a part of our effort to a production of fully conjugated **PPV**s possessing bulky pendants. To determine the minimal steric requirements necessary to prevent of aggregation and to enhance the solubility in organic solvents, we also prepared copolymers with **MEHPPV**. In this paper, we report the synthesis of a new **PPV** derivative containing dendritic phenyl groups on its side chains (**DENPPV**) as an example of highly thermally stable, and TBB defect-free phenyl-substituted **PPV**; in addition, we describe the performance of these polymers as emissive layers in LEDs.

Experimental Section

Materials and Characterization. Bromoxylene, *n*-butyllithium, 2-isopropoxy-4,4,5,5-tetramethyl-1,3,2-dioxaborolane, tetraphenylcyclopentadienone, and 4-bromophenylacetylene were purchased from Aldrich and were used as received. All other solvents were distilled before use. ^{1}H and ^{13}C nuclear magnetic resonance (NMR) spectra were obtained using a Bruker DRX 300 MHz spectrometer. Mass spectra were obtained on a JEOL JMS−SX 102A spectrometer. Fourier transform infrared (FTIR) spectra were acquired using a Nicolet 360 FT-IR spectrometer. Gel permeation chromatographic analyses were performed on a Waters 410 differential refractometer and a Waters 600 controller (Waters Styragel Column). All GPC analyses of polymers were performed in THF solutions at a flow rate of 1 mL/min at 40 °C; the samples were calibrated using polystyrene standards. Thermogravimetric analyses (TGA) and differential scanning calorimetry (DSC) measurements were performed under a nitrogen atmosphere at heating rates of 20 and 10 °C/min, respectively, using Du Pont TGA-2950 and TA-2000 instruments, respectively. UV−vis absorption and photoluminescence (PL) spectra were recorded on an HP 8453 spectrophotometer and a Hitachi F-4500 luminescence spectrometer, respectively. Before investigating the thermal stability of the synthesized polymers, their polymer films were annealed in air at 200 °C for 2 h.

Synthesis of 2-(4,4,5,5-tetramethyl-1,3,2-dioxaborolan-2-yl)xylene. *n*-Butyllithium (1.6 M in hexane, 17.0 mL, 27.09 mmol) was added, by syringe, to a solution of bromoxylene (5.0 g, 28.7 mmol) in THF (100 mL) at −78 °C. The mixture was stirred at −78 °C, warmed to −10 °C for 15 min, and cooled again at −78 °C for 15 min 2-Isopropoxy-4,4,5,5-tetramethyl-1,3,2-dioxaborolane (15.0 g, 80.9 mmol) was added rapidly to the solution, and the resulting mixture was warmed to room temperature and stirred for 24 h. The mixture was poured into water and extracted with ethyl acetate. The organic extracts were washed with brine and dried over magnesium sulfate. The solvent was removed by rotary evaporation and the residue was purified by column chromatography (silica gel, hexane, R_f 0.12) to provide 4.63 g (74%) of the title product. ^{1}H NMR (300 MHz, $CDCl_3$): δ 7.54 (s, 1H), 7.06 (dd, 2H, J = 7.6 Hz), 2.41 (s, 3H), 2.22 (s, 3H), 1.19−1.37 (m, 12H). HRMS: calcd for $C_{14}H_{21}O_2B$, 232.1634; found, 232.1636.

Synthesis of 2,3,4,5-Tetraphenyl-4′-bromophenyl (DEN-Br). A mixture of tetraphenylcyclopentadienone and 4-bromophenylacetylene was refluxed in xylene at 135 °C under nitrogen for 48 h. The reaction mixture was then slowly added into water (150 mL) and extracted with ethyl acetate (3 × 50 mL). The combined extracts were dried ($MgSO_4$), the solvent was evaporated, and the residue was purified by column chromatography (hexane/ethyl acetate, 4:1) to afford **2** (3.23 g, 72%). ^{1}H NMR (300 MHz, $CDCl_3$) δ: 7.62 (s, 1H), 7.35 (d, J = 8.1 Hz, 2H), 7.09−7.14 (m, 4H), 7.02 (d, J = 8.5 2H), 6.87−7.00 (m, 16H). ^{13}C NMR (300 MHz, $CDCl_3$) δ: 142.22, 142.19, 142.00, 141.46, 141.26, 141.13, 140.82, 140.60, 140.45, 140.28, 140.18, 140.12, 139.95, 139.77, 139.67, 135.43, 132.53, 131.95, 131.89, 131.85, 131.67, 131.27, 130.75, 130.45, 130.38, 128.14, 128.09, 127.65, 127.43, 127.19, 127.14, 126.1 0, 121.12. Anal. Calcd for $C_{36}H_{25}Br$: C, 80.59; H, 4.66. Found: C,80.81; H, 4.89. HRMS: calcd for $C_{36}H_{25}Br$, 536.1139; found, 536.1140.

Synthesis of 2′-(2,3,4,5-Tetraphenyl-4′-phenyl)-1,4″-dimethylbenzene (D-CH_3). Suzuki Coupling Reaction. Carefully purified **DEN**Br, (1.0 g 1.84 mmol), 5-(4,4,5,5-tetramethyl-1,3,2-dioxaborolan-2-yl)xylene (0.43 g 1.84 mmol), and $(PPh_3)_4Pd^0$ (1 mol %) were dissolved in a mixture of toluene and 2 M aqueous K_2CO_3 (1.5:1). The solution was placed under a nitrogen atmosphere and heated under reflux with vigorous stirring for 48 h. The mixture was poured into water and extracted with ethyl acetate. The organic extracts were washed with brine and then dried ($MgSO_4$). The solvent was removed by rotary evaporation and the residue was purified by column chromatography (silica gel; 2% ethyl acetate in hexane, R_f 0.3) to provide 650 mg (65%) of the title product. ^{1}H NMR (300 MHz, $CDCl_3$) δ: 7.64 (s, 1H), 7.25 (s, 1H), 7.10−7.18 (m, 10H), 7.02−7.09 (m, 2H), 6.81−6.90 (m, 14H), 2.33 (s, 3H), 2.16 (s, 3H). ^{13}C NMR (300 Hz $CDCl_3$) δ:142.08, 142.07, 142.06, 141.73, 141.12, 140.94, 140.70, 140.38, 140.33, 140.21, 140.12, 139.71, 139.61, 135.43, 132.53, 131.95, 131.89, 131.85, 131.67, 131.27, 130.75, 130.56, 130.33, 128.74, 128.16, 127.93, 127.43, 127.25, 126.97, 126.59, 125.93, 125.67, 21.38, 20.23. Anal. Calcd For $C_{44}CH_{34}$: C, 93.91; H, 6.09. Found: C, 93.91; H, 6.01. HRMS: calcd for $C_{44}H_{34}$, 562.2661; found, 562.2662.

Synthesis of 2-(2,3,4,5-Tetraphenyl-4′-phenyl)-1,4-dibromomethylbenzene (D-CH_2Br). A mixture of D-CH_3, (1.0 g, 1.77 mmol) NBS (0.63 g, 3.55 mmol), and AIBN (0.04 g) was heated under reflux in carbon tetrachloride under nitrogen for 5 days. The reaction mixture was filtered to remove succinimide, the solvent was evaporated, and the residue was purified by column chromatography. ^{1}H NMR (500 MHz, $CDCl_3$), δ: 7.62 (s, 1H), 7.46 (d, J = 7.92 Hz, 1H), 7.34 (d, J = 7.70 Hz, 1H) 7.24−7.15 (m, 10H), 6.94−6.88 (m, 15H), 4.46 (s, 2H), 4.35 (s, 2H).

^{13}C NMR (500 MHz, $CDCl_3$), δ: 142.27, 141.79, 141.66, 141.24, 140.87, 140.25, 139.91, 139.86, 139.51, 139.40, 137.96, 137.36, 135.50, 131.57, 131.52, 131.47, 131.21, 130.83, 129.95, 128.48, 128.15, 127.60, 126.99, 126.93, 126.65, 126.29, 125.74, 125.63, 125.38, 32.72, 31.44. Anal. Calcd for $C_{44}H_{32}Br_2$: C, 73.34; H, 4.48. Found: C, 73.05; H, 4.41. HRMS: calcd for $C_{44}H_{32}Br_2$, 720.0871; found, 720.0848.

General Procedure for the Synthesis of Copolymers. A 1 M solution of potassium *tert*-butoxide in THF was added to a solution of the monomer D-CH_2Br in dry THF at room temperature, and then the mixture was stirred for 4 h. Addition of the THF solution to methanol precipitated the polymer, which was collected, washed with methanol, and stirred with a mixture of methanol and water (1/1) for 1 h. The polymer was again collected, stirred with a mixture of methanol and water (1/1) for 1 h, filtered, washed with methanol, and dried at 60 °C for 24 h.

Device Fabrication and Testing. The electroluminescent (EL) devices were fabricated on an ITO-coated glass substrate that was precleaned and then treated with oxygen plasma before use. A layer of poly(ethylene dioxythiophene):poly(styrenesulfonate) (PEDOT:PSS, Baytron P from Bayer Co.; ca. 40 nm thick) was formed by spin-coating from its aqueous solution (1.3 wt %). The EL layer was spin-coated at 1500 rpm from the corresponding toluene solution (15 mg mL^{-1}) on top of the vacuum-dried PEDOT:PSS layer. The nominal thickness of the EL layer was 65 nm. Using a base pressure below 1×10^{-6} Torr. a layer of Ca (30 nm) was vacuum deposited as the cathode and a thick layer of Al was deposited subsequently as the protecting layer. The current−voltage characteristics were measured using a Hewlett-Packard 4155B semiconductor parameter analyzer. The power of the EL emission was measured using a Newport 2835-C multifunction optical meter. The brightness was calculated using the forward output power and the EL spectra of the devices; a Lambertian distribution of the EL emission was assumed.

Results and Discussion

The dendritic phenyl substitute, 2,3,4,5-tetraphenyl-4′-bromophenyl, was synthesized according to Scheme 1. Suzuki coupling of xylene boronic acid with 2,3,4,5-tetraphenyl-4′-bromophenyl in toluene, in the presence

Scheme 1. Synthesis of Dendritic Phenyl Bromide

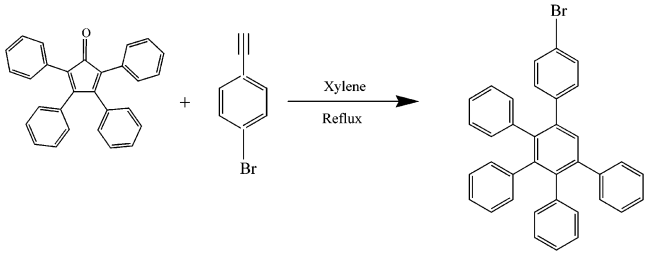

of tetrakis(triphenylphosphine)palladium(0) as catalyst, gave the dendritic phenyl-substituted xylene derivative. The dendritic phenyl-substituted dibromo monomer (**D-CH$_2$Br**) was synthesized by bromination of 2′-(2,3,4,5-tetraphenyl-4′-phenyl)-1,4″-dimethylbenzene with NBS, using AIBN as the radical initiator. The polymers were prepared according to Scheme 2.

The copolymers were prepared using comonomer feed ratios of **D-CH$_2$Br** and 2-methoxy-5-(2-ethyl)hexyloxy-1,4-bis(bromomethyl)benzene of 100:00, 88:12, 75:25, 63:37, 50:50, 25:75, and 0:100; we name the corresponding copolymers **DENPPV**, **88DENPPV**, **75DENPPV**, **63DENPPV**, **50DENPPV**, **25DENPPV**, and **MEH-PPV**, respectively. Figure 1 displays the FTIR spectra of **DENPPV** and **MEHPPV**. The absorption bands that appear at 1581−1596 cm^{-1}, are characteristic of C=C bonds. The absorption bands at 3056 and 961 cm^{-1} are due to stretching modes for the vinylene C=C bond and C−H out-of-plane bending, respectively, of the trans configuration. The ^{1}H NMR and ^{13} C H NMR spectra of **DENPPV** have been presented as Supporting Information. The aromatic and vinyl protons appear within the range of 7.60−6.84 ppm. **PPV**s containing TBB defect (head-to-head (H−H) or tail to tail (T−T) couplings, that are formed as the result of a side reactions[4,20] are responsible for the CH_2–CH_2 groups that present the peaks at 2.5−2.9 ppm. We did not observe peaks for H−H couplings in the ^{1}H NMR spectrum of the obtained polymer. It is clear that this side reaction is suppressed because of (i) the electronic effect arising from the stronger acidity of the bromomethyl moiety at the ortho position of the dendritic phenyl group and (ii) the steric effect of the substituting dendritic phenyl group. We

Scheme 2. Synthesis of DEN PPV and Copolymers

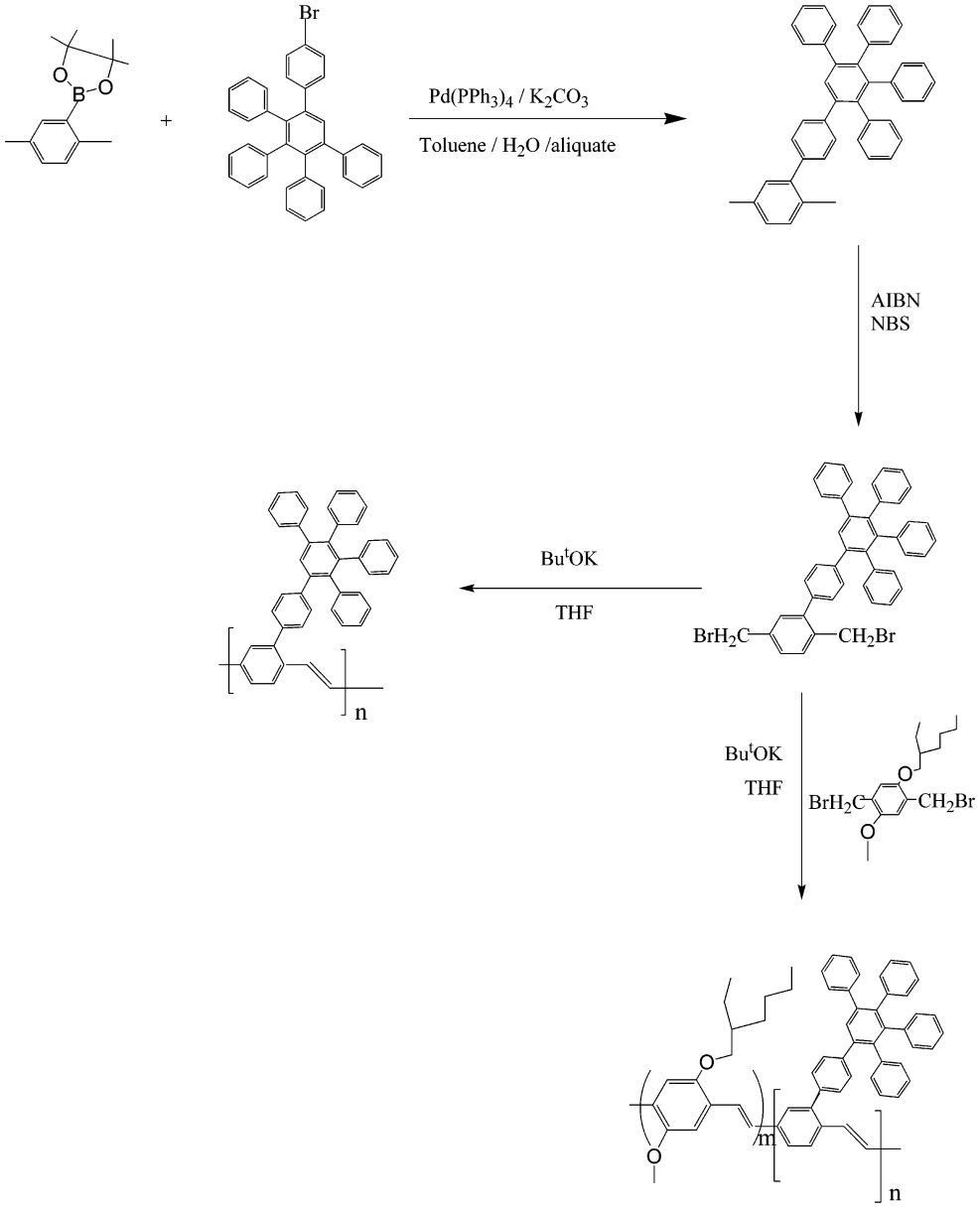

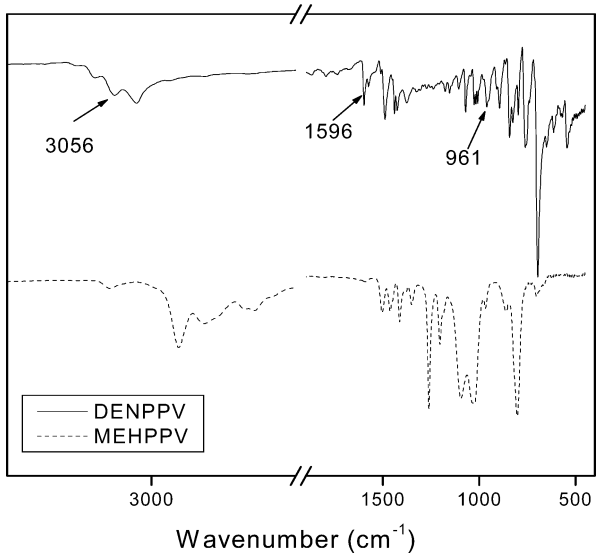

Figure 1. IR spectra of **DENPPV** and **MEHPPV**.

Table 1. Molecular Weights and Thermal Properties of DENPPV and Copolymers

polymer	mol wt[c] M_n	mol wt[c] M_w	PDI[a]	T_g (°C)[b]	TGA 5 wt % loss temp (°C)
DENPPV	100 000	280 000	2.1	243	502
88DENPPV	120 000	173 000	1.5	226	468
75DENPPV	110 600	136 000	1.1	208	448
63DENPPV	98 000	188 000	1.9	198	427
50DENPPV	78 000	110 000	1.5	186	398
25DENPPV	95 000	238 000	2.0	145	389

[a] PDI = Polydispersity index. [b] T_g = Glass transition temperature. [c] Molecular weights were calculated with relative to polystyrene standard.

measured the molecular mass and polydispersity index (PDI) of each copolymer by GPC using THF as the eluent; the results are presented in Table 1. We determined the weight-average molecular weights of the polymers to be in the range $(1.6-3) \times 10^5$ with polydispersities ranges from 1.1 to 2.1. The **DENPPV** polymer exhibits limited solubility in THF and in DMF, and it has very low solubility when its molecular weight reaches above 3×10^5. The glass transition temperature (T*g*) of **DENPPV** occurs at 243 °C, which is much higher than that of **MEHPPV**, that can extended device longevity.[21,22] TGA of the **DENPPV** copolymers displayed that their 5% weight losses occurred between 502 and 336 °C. These thermal stabilities and glass transition temperatures are higher than those of other phenylated **PPV**s reported previously. The higher glass transition and thermal stability are due to the restricted polymer chain mobility and resistant to thermal oxidation imparted by the rigid dendritic phenyl group.

The PL spectrum of the dendritic phenyl exhibits a peak maximum at 370 nm (Figure 2a), while the maximum absorption peak due to the $\pi-\pi$ transition of the backbone of **DENPPV** appeared at 423 nm. A large overlapped area from the two respective peaks is present indicating the possible intramolecular energy transfer since it is known that energy transfer can occur readily when the PL of a chromophore having a wide band gap overlaps with the electronic absorption of the other chromophore possessing a narrow one. We measured the energy band gap of the polymers using the oxidation and reduction potentials obtained from cyclic voltammetry and the UV−vis absorption spectra. The

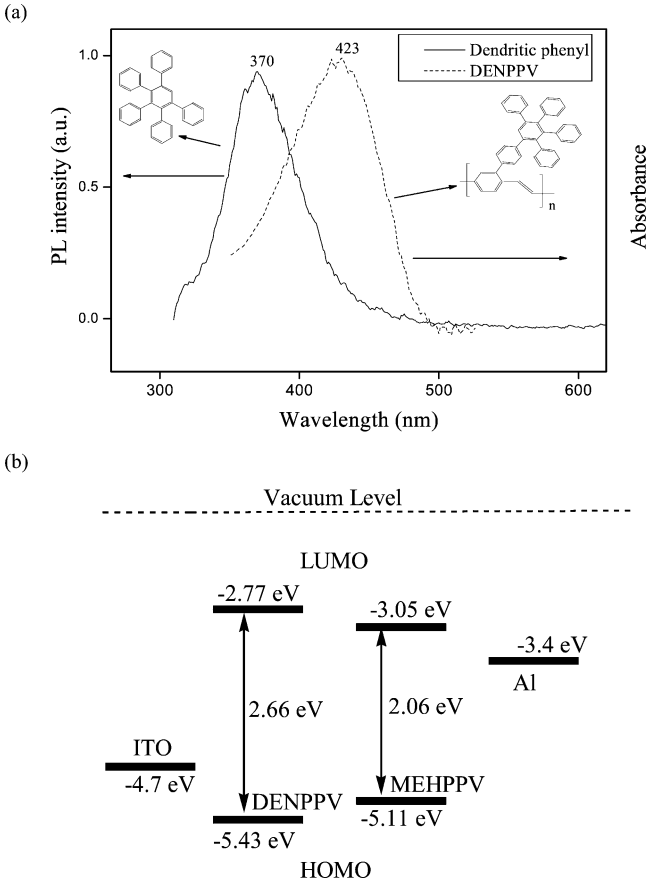

Figure 2. (a) UV and PL spectra of the **DENPPV** and a dendritic phenyl model compound and (b) energy level diagram of **DENPPV** and **MEHPPV**.[26]

reduction (E_{red}) and oxidation (E_{ox}) potentials for **DENPPV** were 1.63 and 1.13, respectively. The highest occupied and lowest unoccupied molecular orbital (HOMO and LUMO) energies were estimated electrochemically to be −5.43 and −2.77 eV, respectively, with a band gap of 2.66 eV. Figure 2b presents the energy level diagram of **DENPPV** and **MEHPPV**. The LUMO of **DENPPV** is higher than that of **MEHPPV**, while the HOMO of **DENPPV** is lower than that of **MEHPPV**. From Figure 2, parts a and b, we conclude that intramolecular energy transfer can occur effectively from the phenylated dendrimer units to the polymer backbone.

The UV and PL spectra of the polymers in THF solution are presented in Figure 3. The absorption peak maximum of each polymer appears between 423 and 485 nm. The polymer solutions display intense blue-green emissions (peak maxima at 492−551 nm), which are blue-shifted as the concentration of the dendritic phenyl monomer in the copolymer increased. The **DENPPV** polymer displays an emission maximum at 492 nm and a shoulder peak in the range 520−550 nm. We attribute the shoulder peak that appears in the PL spectrum of **DENPPV** to the vibronic effect of the aromatic ring of the substituent phenylated dendrimer, because these two peaks differ by 1100−1200 cm^{-1}, calculated using peak maximum values of PL spectrum.[23] Surprisingly, this shoulder peak was not prominent in the PL spectra of the copolymers. On the other hand, the emission at 598 nm, which is due to aggregation appeared in the spectra of **MEHPPV** and **25DENPPV**. In Figure 3, we observe that excimer formation is suppressed significantly upon increasing the content of dendritic phenyl monomer in **MEHPPV**.

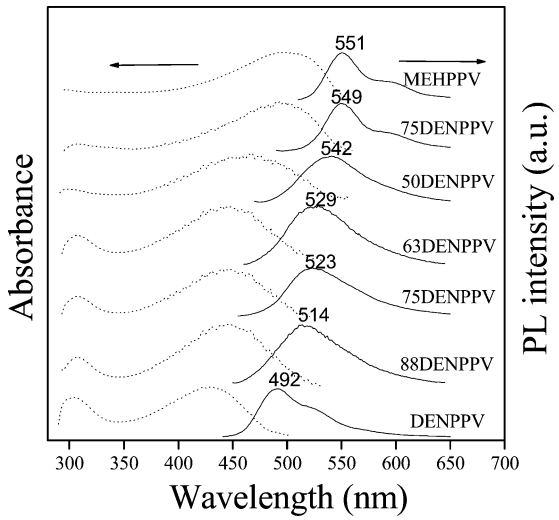

Figure 3. UV and PL spectra of **DENPPV** and copolymers.

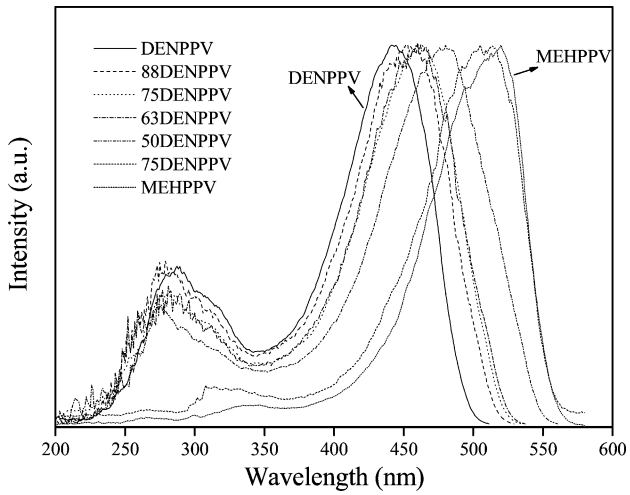

Figure 4. Excitation spectra of the copolymers in THF solution.

Figure 4 presents the excitation spectra of the polymers in solution; they indicate that the well-resolved small peak at 300 nm is due to the substituent dendritic phenyl group, which also confirms that energy transfer occurs from the side chain to the polymer backbone. We observe from Figure 4 that the excitation spectra are the same as the UV−vis spectra; this finding indicates the high purity of the emitting chromophores.

The thin film PL spectra was observed to be similar to those of the solutions, e.g., **DENPPV** undergoes no significant red shift in the film. In contrast, the **MEH-PPV**, lacking dendron substituents exhibits a marked red shift in its solid state from its solution state absorption and emission spectra (551 vs 582 nm), which we believe can be attributed to interactions, such as $\pi-\pi$ stacking, between the chromophores. These spectra also suggest that the aggregation and migration of the chromophores are reduced in the dendrimers and indicate that even the first-generation dendrimers can effectively suppress $\pi-\pi$ stacking among polymer chains. Table 2 presents the quantum yields of polymers in the solid state and in solution, and their photoluminescence data. The decadic molar extinction coefficient (ϵ) was determined in THF using eq 1:

$$\epsilon = \mathrm{OD}/cl \ (\mathrm{dm^3\ mol^{-1}\ cm^{-1}}) \qquad (1)$$

Table 2. Absorption and Photoluminescence Data of DENPPV and Copolymers

polymer	ϵ (M^{-1} cm^{-1})[a]	OD[b]	L (nm)[c]	M (mol/cm^3)[d]	η^{s} [e]	η^{tf} [f]
DENPPV	72 900	0.241 47	65	5.04	0.67	0.65
88DENPPV	11 920	0.0855	45	3.09	0.66	0.68
75DENPPV	60 070	0.0862	52	2.75	0.55	0.82
63DENPPV	21 506	0.167 58	65	2.07	0.47	0.41
50DENPPV	52 185	0.169 08	60	5.33	0.50	0.42
25DENPPV	92 065	0.4284	45	1.33	0.33	0.30
MEHPPV	99 274	0.140 78	85	1.48	0.30	0.27

[a] ϵ = Decadic molar extinction coefficient (dm^3 mol^{-1}cm^{-1}). [b] OD = Absorbance or optical density in the solid state. [c] L = Thickness of the thin film. [d] M = Fluorescent chromophore concentration in the film of each composite. [e] η^{tf} = Thin-film quantum yield estimated by using coumarin 6 dispersed in PMMA film at a concentration $<10^{-3}$ M.[25] [f] η^{s} = Solution quantum yield estimated by using coumarin 6 in THF as the reference.

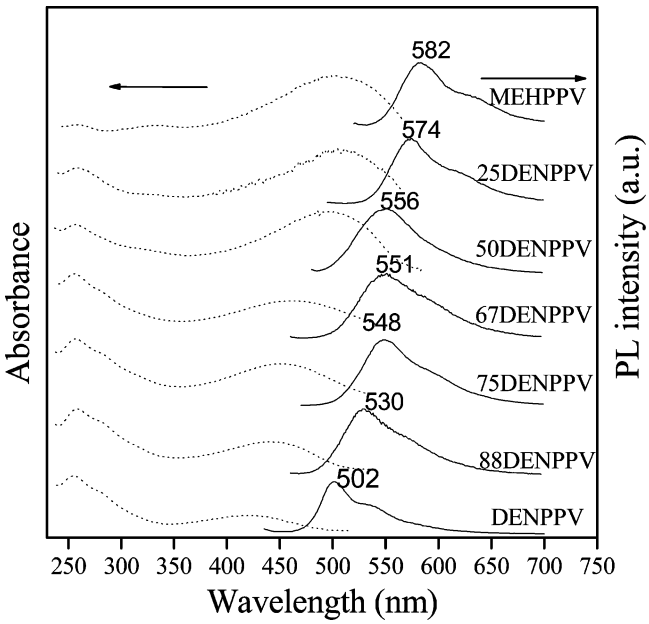

Figure 5. UV and PL spectra of **DENPPV** and copolymer thin films.

where OD is the optical density, c is the concentration of the polymer in solution, and l is the optical path length of the sample. We determined the fluorescent chromophore concentration (M) in the thin film using eq 2:

$$M = \mathrm{OD}/\epsilon L \ (\mathrm{mol/cm^3}) \qquad (2)$$

where L is the thickness of the film.

DENPPV displays a quantum yield of 0.67 in THF, calculated with reference to coumarin 6; this quantum yield is for about 2-fold higher than that of the well-established **MEHPPV**, in the solid state it is 0.65. The copolymer **75DENPPV** displays a higher quantum yield (0.82) in the solid state than that of **DENPPV**, which can be explained by quantum confinement.[24] The higher quantum yields of copolymers **88DENPPV** and **75 DENPPV** in their solid state than that of solution can be explained as being due to the steric effect of dendritic phenyls where the **PPV** backbone forces the pendant dendritic phenyl ring to point away (one up and one down) from the conjugated plane. Such a three-dimensional structure prevents **PPV** stacking in any dimension, providing higher quantum yields.[10d]

We fabricated double-layer LED devices having the configuration ITO/poly(3,4-ethylenedioxythiophene) (PE-

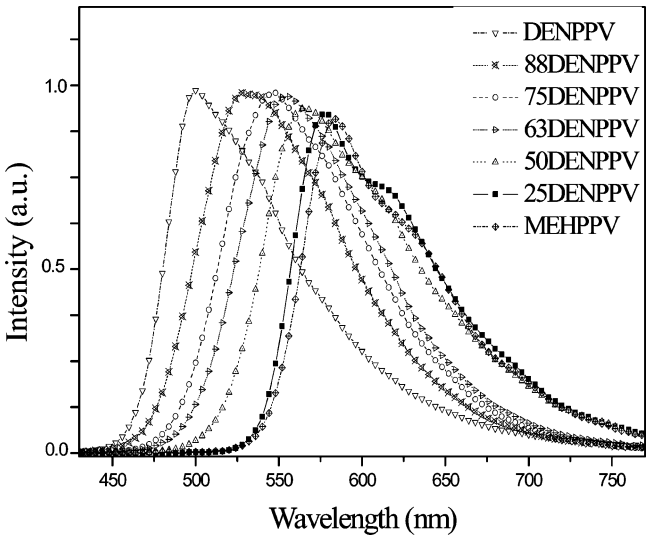

Figure 6. EL spectra of **DENPPV** and copolymers.

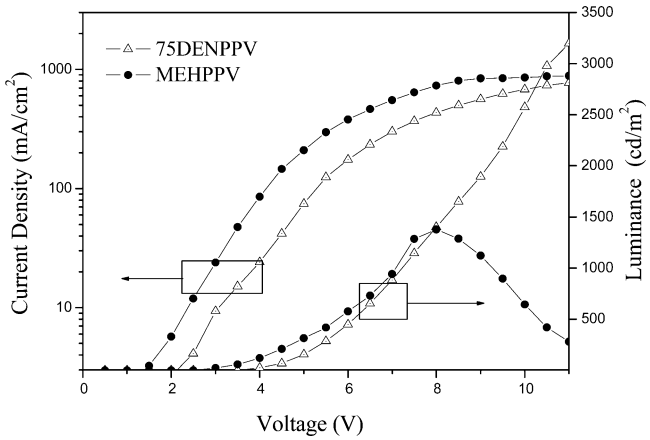

Figure 7. Plots of current density vs voltage and luminescence vs voltage of the devices prepared from **75DENPPV** and **MEHPPV**.

DOT):poly(styrene sulfonic acid) (PSS)/**DENPPV**/Ca/Al. The EL spectrum of the **DENPPV** device was similar to its PL spectrum in that it displays an intense signal having a peak maximum at 499 nm (Figure 6.). The copolymer **MEHPPV/DENPPV** at a molar ratio of 25/75 exhibits an even more intense signal at 547 nm. Figure 7 presents the variations of the current density and brightness of the EL devices prepared from **MEHPPV** and **75DENPPV**. The electroluminescence of copolymer **75DENPPV** displays highest efficiency (0.12 lm/W), it is 70% higher than that of **MEHPPV** (0.07 lm/W) measured under similar conditions. All of these polymers shows better electroluminescence efficiency (η_{EL}) providing that a minimization of the self-quenching has occurred by attaching the bulky dendrons on the polymer backbone and by preventing aggregation of the polymer chains without altering their electronic properties and better device structure.

Conclusion

In this study, we synthesized a high molecular-weight poly(phenylenevinylene) (**PPV**) containing bulky dendritic phenyl groups (**DENPPV**) as **PPV** side chains. The dendritic phenyl-substituted monomer was synthesized through Suzuki coupling reaction and then polymerized using the Gilch route. The dendritic phenyl group is found to involved in the intramolecular energy transfer that occurs from the dendritic phenyl groups to the **PPV** backbone. The PL quantum yield of **DENPPV** (67%) is among the highest values reported for fully conjugated **PPV**. The copolymer **DENPPV/MEHPPV** molar ratio of 75/25 exhibited increased values of η_{EL} and η_{PL} that may make them useful as active layers in devices such as LEDs and photovoltaic diodes.

Supporting Information Available: ^{1}H NMR and ^{13}C NMR spectra of **DENPPV** and the monomer. This material is available free of charge via the Internet at http://pubs.acs.org.

Acknowledgment. The authors thank the National Science Council, Taiwan, for financial support through NSC 92-2120-M-009-009.

References and Notes

(1) (a) Yang, Z.; Karasz, F. E.; Geise, H. J. *Macromolecules* **1993**, *26*, 6570. (b) Strukelj, M.; Papadimitrakopoulos, F.; Miller, T. M. *Science* **1995**, *267*, 1969. (c) Grem, G.; Leditzky, G.; Ullrich, B.; Leising, G. *Adv. Mater.* **1992**, *4*, 3621. (d) Berggren, M.; Inganäs, O.; Gustafsson, G.; Carberg, J. C.; Rasmusson, J.; Anderson, M. R.; Hjertberg, T.; Wennerstron, O. *Nature* **1994**, *372*, 444.

(2) (a) Greenham, N. C.; Samuel, I. D. W.; Hayes, G. R.; Phillips, R. T.; Kessener, Y. A. R. R.; Moratti, S. C.; Holmes, A. B.; Friend, R. H. *Chem. Phys. Lett.* **1995**, *241*, 89. (b) Samuel, I. D. W.; Rumbles, G.; Collison, C. J.; Crystall, B.; Moratti, S. C.; Holmes, A. B. *Synth. Met.* **1996**, *76*, 15. (c) Gettinger, C. L.; Heeger, A. J.; Drake, J. M.; Pine, D. J. *J. Chem. Phys.* **1994**, *101*, 1673. (d) Hwang, D.-H.; Kim, S. T.; Li, X. C.; Chuah, B. S.; Demello, J. C.; Friend, R. H.; Moratti, S. C.; Holmes, A. B. *Polym. Prepr.* **1997**, *38*, 319.

(3) (a) Bao, Z.; Peng, Z.; Galvin, M. E.; Chandross, E. A. *Chem. Mater.* **1998**, *10*, 1201. (b) Chung, S. J.; Kwon, K. Y.; Lee, S. W.; Jin, J. I.; Lee, C. H.; Lee, C. E.; Park, Y. *Adv. Mater.* **1998**, *10*, 1112. (c) Chen, Z. K.; Meng, H.; Lai, Y. H.; Huang, W. *Macromolecules* **1999**, *32*, 4351. (d) Greenham, A. C.; Morrati, S. C.; Bradley, D. D. C.; Friend, R. H.; Burn, P. L.; Holmes, A. B. *Nature (London)* **1993**, *365*, 628.

(4) Becker, H.; Spreitzer, H.; Kreuder, W.; Kluge, E.; Schenk, H.; Parker, I.; Cao, Y. *Adv. Mater.* **2000**, *12*, 42.

(5) Sokolik, I.; Yang, Z.; Karasz, F. E.; Morton, D. C. *J. Appl. Phys.* **1993**, *74,* 3584. (b) Yang, Z.; Karasz, F. E.; Geise, H. J. *Macromolecules* **1993**, *26*, 6570. (c) Pasco, S. T.; Lahti, P. M.; Karasz, F. E. *Macromolecules* **1999**, *32*, 6933. (d) Mikroyannidis, J. A. *Chem. Mater.* **2003**, *15,* 1865.

(6) Gustafsson, G.; Cao, Y.; Treacy, G. M.; Klavetter, F.; Colaneri, N.; Heeger, A. J. *Nature* **1992**, *357*, 477.

(7) Aratani, S.; Zhang, C.; Pakbaz, K.; Hoger, S.; Wudl, F.; Heeger, A. J. *J. Elec. Mater.* **1993**, *22*, 745.

(8) Yang, Y.; Heeger, A. J. *Appl. Phys. Lett.* **1994**, *64*, 1245.

(9) Braun, D.; Heeger, A. J. *Appl. Phys. Lett.* **1991**, *58*, 1982.

(10) (a) Chu, H. Y.; Hwang, D.-H.; Do, L.-M.; Chang, J.-H.; Shim, H.-K.; Holmes, A. B.; Zyung, T. *Synth. Met.* **1999**, *101*, 216. (b) Hsieh, B. R.; Yu, Y.; Forsythe, E. W.; Schaaf, G. M.; Feld, W. A. *J. Am. Chem. Soc.* **1998**, *120*, 231. (c) Lee, S. H.; Jang, B.-B.; Tsutsui, T. *Chem. Lett.* **2000**, 1184. (d) Peng, Z.; Zhang, J.; Xu, B. *Macromolecules* **1999**, *32*, 5162.

(11) (a) Andersson, M. R.; Yu, G.; Heeger, A. J. *Synth. Met.* **1997**, *885*, 1275. (b) Wudl, F.; Srdanov, G.; US Patent No. 5 189 136, **1993.**

(12) Johansson, D. M.; Xiangjun Wang; Tomas Johansson; Inganas, O.; Yu, G.; Srdanov, G.; Andersson, M. R. *Macromolecules* **2002**, *35,* 4997.

(13) Becker, H.; Spreitzer, H.; Kreuder, W.; Kluge, E.; Vestweber, H.; Schenk, H.; Treacher, K. *Synth.* Met. **2001**, *122*, 105.

(14) Johansson, D. M.; Theander, M.; Srdanov, G.; Yu, G.; Inganas, O.; Andersson, M. R. *Macromolecules* **2001**, *34*, 3716.

(15) Klarner, G.; Miller, R. D.; Hawker, C. J. *Polym. Prepr.* **1998**, *39*, 1006.

(16) Frauenrath, H. *Prog. Polym. Sci.* **2005**, *30* 325.

(17) Chou, C.-H.; Hsu, S. L.; Dinakaran, K.; Chiu, M. Y.; Wei, K. H. *Macromolecules* **2005**, *35*, 745. (b) Chou, C.-H.; Shu, C.-F. Macromolecules **2002**, *35,* 9673.
(18) Qu, J.; Zhang, J.; Grimsdale, A. C.; Mu1len, K.; Jaiser, F.; Yang, X.; Neher, D. *Macromolecules* **2004**, *37*, 8297.
(19) Pogantsch, A.; Wenzel, F. P.; List, E. J. W.; Leising, G.; Grimsdale, A. C.; Mullen, K. *Adv. Mater.* **2002**, *14*, 1061.
(20) Becker, H.; Spreitzer, H.; Ibrom, K.; Kreuder, W. *Macromolecules* **1999**, *32*, 4925.
(21) Dogariu, A.; Gupta, R.; Heeger, A. J.; Wang, H. *Synth. Met.* **1999**, *100*, 95.
(22) Shin, D. C.; Ahn, J. H.; Kim, Y. H.; Kwon, S. K. *J. Polym. Sci., Part A: Polym. Chem.* **2000**, *38*, 3086.
(23) Chen, S. H.; Su, A. C.; Chou, H. L.; Peng, K. Y.; Chen, S. A. *Macromolecules* **2004**, *37*, 167.
(24) Johansson, D. M.; Srdanov, G.; Yu, G.; Theander, M.; Inganas, O.; Andersson, M. R. *Macromolecules* **2000**, *33*, 2525.
(25) Swanson, S. A.; Wallraff, G. M.; Chen, J. P.; Zhang, W.; Bozano, L. D.; Carter, K. R.; Salem, J. R.; Villa, R.; Scott, J. C. *Chem. Mater.* **2003**, *15,* 2305.
(26) Jin, S. H.; Jang, M. S.; Suh, H. S.; Cho, H. N.; Lee, J. H.; Gal, Y. S. *Chem. Mater.* **2002**, *14,* 643.

MA050252Q

Enhanced Luminance and Thermal Properties of Poly(phenylenevinylene) Copolymer Presenting Side-Chain-Tethered Silsesquioxane Units

Chia-Hung Chou, So-Lin Hsu, Siao-Wei Yeh, Hsu-Shen Wang, and Kung-Hwa Wei*

Department of Materials Science and Engineering, National Chiao Tung University, Hsinchu, Taiwan 30049, R.O.C.

Received May 24, 2005; Revised Manuscript Received August 17, 2005

ABSTRACT: We have synthesized, using the Gilch polymerization method, a new series of high-brightness, soluble copolymers (POSS-PPV-*co*-MEHPPV) of poly(*p*-phenylenevinylene) (PPV) containing side-chain-tethered polyhedral oligomeric silsesquioxane (POSS) pendent units and poly(2-methoxy-5-[2-ethylhexyloxy]-1,4-phenylenevinylene) (MEHPPV). This particular molecular architecture of POSS-PPV-*co*-MEHPPV copolymers possesses not only a larger quantum yield (0.85 vs 0.19) but also higher degradation and glass transition temperatures relative to those of pure MEHPPV. The maximum brightness of a double-layered-configured light-emitting diode (ITO/PEDOT/emissive polymer/Ca/Al) incorporating a copolymer of MEHPPV and 10 mol % PPV-POSS was 5 times as large as that of a similar light-emitting diode incorporating pure MEHPPV (2196 vs 473 cd/m^2).

Introduction

Emissive media based on electroluminescent (EL) polymers are currently under development for a number of display applications,[1−4] including large-area flat-panel displays that can be driven at low voltage. Polymer light-emitting diodes (PLEDs) are very promising candidates for the development of low-cost, multicolored, large-area flat-panel displays because their molecular structures are readily modified and because they can be handled using a range of wet processing techniques.[5,6] A number of issues remain to be resolved, however, before commercialization of these devices can occur. The formation of excimers resulting from the aggregation of their molecular chains in the solid state, and rather short operating lifetimes, owing to their low thermal stabilities. Several attempts have been made to reduce the formation of aggregates of polymer chains in the solid state. One such approach is the introduction of bulky organic units into the side chains of the polymer. This tactic has been used, for example, in the case of poly(*p*-phenylenevinylene) (PPV)-based alternating copolymers containing conjugated phenylenevinylene segments and nonconjugated spacers;[7−9] these bulky side groups disrupt the packing of the polymer chains, which results in the formation of amorphous PPVs displaying reduced aggregation. Another approach to improving the efficiency of the devices is to blend hole-transporting and electron-transporting materials to balance the injected charges.[10−12a] When such a device is operated for a long time, however, this method can cause some defect to occur in some cases.[12b−d] Other approaches include improving the antioxidative properties of the pendant groups or chain ends[13] and limiting chain mobility by blending[14] with a high-T_g polymer. One approach to not only preventing polymer chains from aggregating but also improving the antioxidative properties of their pendent groups is to use inorganic pendent groups as the side chains of the conjugated polymers.

The chemistry of polyhedral oligomeric silsesquioxane (POSS) covalently bonded to organic polymers has been developed recently. One set of members of the polyhedral oligomeric silsesquioxane family are octamers having the general formula $(RSiO_{1.5})_8$; they consist of a rigid, cubic silica core having a nanopore diameter of ca. 0.3−0.4 nm.[15] The incorporation of $(RSiO_{1.5})_8$ into some polymers leads to an enhancement of their thermal stability and mechanical properties.[16−18]

The first study in which POSS and conjugate polymers were combined involved tethering POSS to the chain ends of poly(2-methoxy-5-[2-ethylhexyloxy]-1,4-phenylenevinylene) (MEHPPV)[19] and the luminescent polymer poly(9,9′-dioctylfluorene) (PFO). The enhanced electroluminescence of these nanostructured polymers was attributed to POSS, imparting a reduction in the degree of either aggregation or excimer formation.[13] The approach of tethering POSS at the ends of a polymer's chain, however, limits the number of POSS units that can be attached. In a previous study, we synthesized a series of side-chain-tethered POSS derivatives of polyimide as a method of lowering its dielectric constant.[20] More recently, side-chain-tethered PF−POSS copolymers have been synthesized; they display a stronger and purer blue electroluminescence.[21a] In this paper, we report a new series of asymmetric PPV derivatives presenting POSS units in their side chains. We synthesized these polymers using the Gilch polymerization method. We incorporated the POSS units into the PPV to improve its thermal stability and EL characteristics. The bulky silsequioxane group was introduced at the meta position of the phenyl substitutents to inhibit intermolecular interactions between the resulting polymer chains. Such meta substitution also helps to provide an amorphous state and better processability. To the best of our knowledge, the introduction of an inorganic side group, such as POSS, into PPV-based alternating

* Corresponding author: Tel 886-35-731871, Fax 886-35-724727, e-mail khwei@cc.nctu.edu.tw.

10.1021/ma051055u CCC: $30.25
Published on Web 10/07/2005

Scheme 1.[a] **Synthesis of POSS-PPV-*co*-MEHPPV Copolymers**

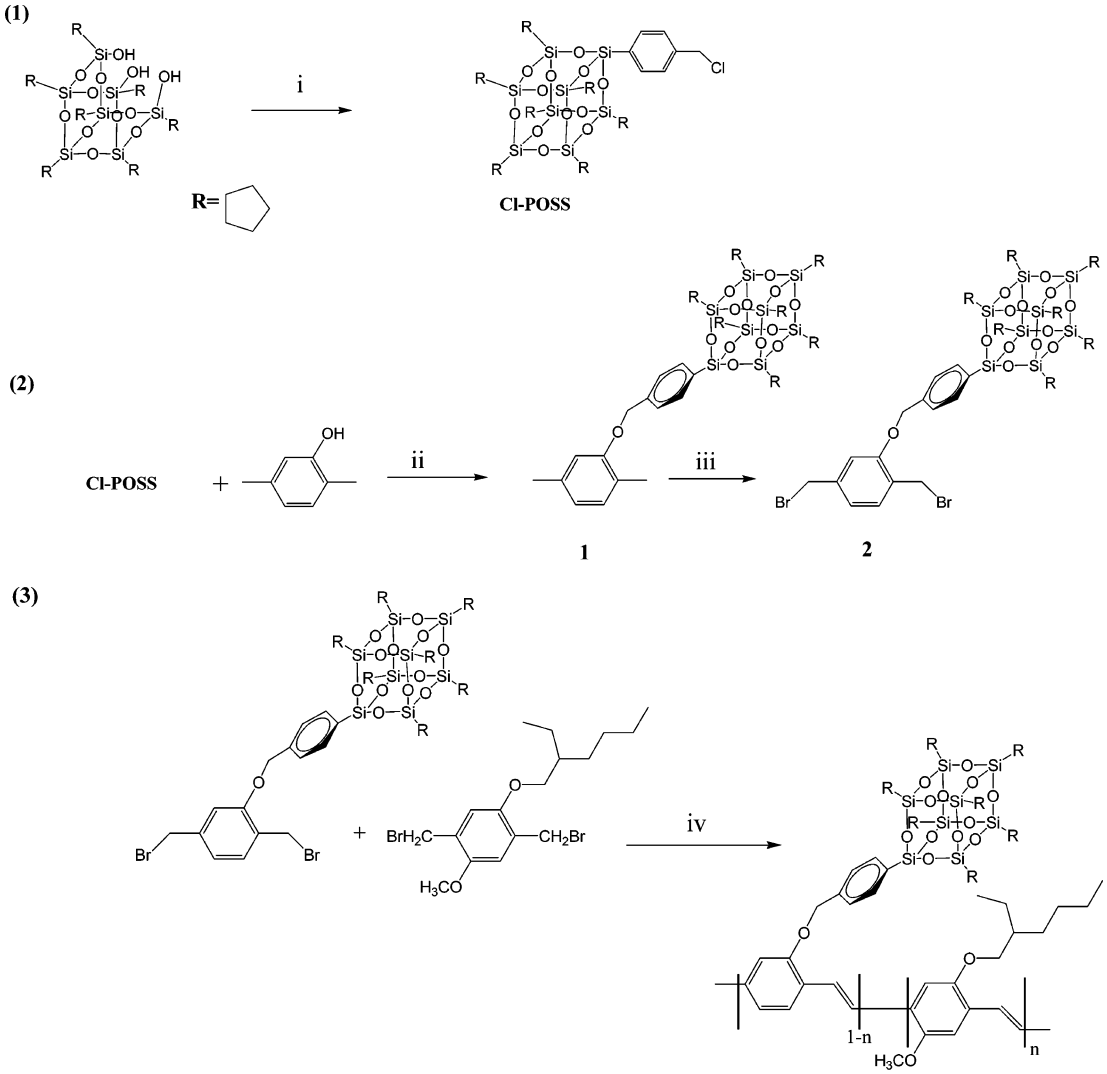

[a] Reagents and conditions: i, trichloro[4-(chloromethyl)phenyl]silane, $HNEt_3Cl$; ii, K_2CO_3, DMF/THF; iii, *N*-bromosuccinimide (NBS)/AIBN/CCl_4; iv, *tert*-BuOK/THF.

copolymers has not yet been described. We believe that developing POSS/poly(*p*-phenylenevinylene) copolymers having well-defined architectures will allow its luminescence properties to be tailored more precisely through modifications of its molecular structure.

Experimental Section

Chlorobenzylcyclopentyl-POSS[19a] was synthesized according to literature procedures. THF was distilled under nitrogen from sodium benzophenone ketyl; other solvents were dried using standard procedures. All other reagents were used as received from commercial sources, unless otherwise stated.

Chlorobenzylcyclopentyl-POSS. ^{1}H NMR (300 MHz, $CDCl_3$): δ 7.64 (d, J = 8.1 Hz, 2H), 7.37 (d, J = 8.1 Hz, 2H), 4.57 (s, 2H), 2.26−1.21 (m, 56H), 1.16−0.81 ppm (m, 7H). ^{29}Si NMR (600 MHz, THF): −67.8, −68.2, −79.6 ppm.

Synthesis of POSS-CH_3 (1). 2,5-Dimethylphenol (238 mg, 1.95 mmol) was stirred with K_2CO_3 (4.58 g, 33.18 mmol) and KI (1.57 g, 9.48 mmol) in DMF (30 mL) and THF (15 mL) at room temperature for 1 h. A small amount of Cl-POSS (2.0 g, 1.95 mmol) was added, and then the whole mixture was heated at 70 °C for 3 h. The reaction mixture was then slowly poured into water (300 mL) and extracted with chloroform (3 × 50 mL). The combined extracts were dried ($MgSO_4$), the solvents were evaporated, and the residue was purified by column chromatography (hexane/chloroform, 1:10) to afford **1** (1.86 g, 81%). ^{1}H NMR (300 MHz, $CDCl_3$): δ 7.70 (d, J = 8.1 Hz, 2H), 7.51−7.31 (b, 3H), 7.03 (d, J = 6.9 Hz, 1H), 6.67 (s, 1H), 5.09 (s, 2H), 2.37 (s, 3H), 2.32 (s, 3H), 2.27−1.21 (m, 56H), 1.17−0.81 ppm (m, 7H).

Synthesis of POSS-CH_2Br (2). A mixture of POSS-CH_3 (**1**; 600 mg, 0.510 mmol), NBS (198.6 mg, 1.02 mmol), and AIBN (8.0 mg) was heated under reflux in carbon tetrachloride under nitrogen for 3 h. The reaction mixture was filtered to remove succinimide, the solvent was evaporated, and the residue was purified by column chromatography (hexane/chloroform, 1:10). ^{1}H NMR (300 MHz, $CDCl_3$) δ: 7.73 (d, J = 8.1 Hz, 2H), 7.59 (d, J = 6.9 Hz, 1H), 7.38 (d, J = 8.1 Hz, 2H), 7.09 (d, J = 6.9 Hz, 1H), 7.01 (s, 1H), 5.18 (s, 2H), 4.73 (s, 2H), 4.57 (s, 2H), 2.26−1.21 (m, 56H), 1.16−0.81 ppm (m, 7H). Anal. Calcd for $C_{50}H_{76}Br_2O_{13}Si_8$ (%): C, 47.30; H, 6.03. Found: C, 47.18; H, 6.09.

General Procedure for the Synthesis of Copolymers POSS−PPV-*co*-MEHPPV. A solution of potassium *tert*-butoxide (1 M in THF) was added to a solution of the monomer in dry THF, and then the mixture was stirred for 4 h. End-group capping was performed by heating the solution under reflux for 1 h in the presence of tetrabutylbenzyl bromide. Addition of the THF solution to methanol precipitated the polymer, which was collected, washed with methanol, and stirred in a mixture of methanol and water (1:1) for 1 h. The polymer was collected, washed with methanol, filtered, and dried at 50 °C for 24 h. After cooling, the polymer was recovered by precipitating it into a mixture of methanol and acetone (4:1). The crude polymer was collected, purified twice

Table 1. Physical Properties of the POSS-PPV-*co*-MEHPPV Copolymers

	T_g (°C)	T_d[a] (°C)	M_n	M_w	PDI	yield (%)
MEHPPV	71	370	61 000	111 000	1.82	78
POSS-PPV1-*co*-MEHPPV	90	381	55 000	107 000	1.95	66
POSS-PPV3-*co*-MEHPPV	96	395	52 000	98 000	1.88	64
POSS-PPV5-*co*-MEHPPV	*b*	417	48 000	91 000	1.90	69
POSS-PPV10-*co*-MEHPPV	*b*	453	39 000	73 000	1.87	60

[a] Temperature at which 5% weight loss occurred, based on the initial weight. [b] The glass transition disappeared because of the steric hindrance imposed on the main molecular chains by the POSS units.

by reprecipitation from THF into methanol, and subsequently dried under vacuum at 50 °C for 24 h. The ^{1}H and ^{13}C NMR spectra of MEHPPV and PPV−POSS appear to be identical because of the low content of POSS in the latter polymer.

Characterization. ^{1}H, ^{13}C, and ^{29}Si nuclear magnetic resonance (NMR) spectra of the compounds were obtained using a Bruker DRX 300 MHz spectrometer. Mass spectra of the samples were obtained on a JEOL JMS-SX 102A spectrometer. Fourier transform infrared (FTIR) spectra of the synthesized materials were acquired using a Nicolet 360 FT-IR spectrometer. Gel permeation chromatographic analyses were performed on a Waters 410 differential refractometer and a Waters 600 controller (Waters styragel column). All GPC analyses of polymers in THF solutions were performed at a flow rate of 1 mL/min at 40 °C; the samples were calibrated using polystyrene standards. Thermogravimetric analysis (TGA) and differential scanning calorimetry (DSC) measurements were performed under a nitrogen atmosphere at heating rates of 20 and 10 °C/min, respectively, using Du Pont TGA-2950 and TA-2000 instruments, respectively. UV−vis absorption and photoluminescence (PL) spectra were recorded on a HP 8453 spectrophotometer and a Hitachi F-4500 luminescence spectrometer, respectively. Before investigating the thermal stability of the synthesized polymers, their polymer films were annealed in air at 200 °C for 2 h.

Device Fabrication and Testing. The electroluminescent (EL) devices were fabricated on an ITO-coated glass substrate that was precleaned and then treated with oxygen plasma before use. A layer of poly(ethylenedioxythiophene):poly(styrenesulfonate) (PEDOT:PSS, Baytron P from Bayer Co.; ca. 40 nm thick) was formed by spin-coating it from an aqueous solution (1.3 wt %). The EL layer was spin-coated, at 1500 rpm from the corresponding toluene solution (15 mg mL^{-1}), on top of the vacuum-dried PEDOT:PSS layer. The nominal thickness of the EL layer was 65 nm. Using a base pressure below 1×10^{-6} Torr, a layer of Ca (35 nm) was vacuum-deposited as the cathode, and a thick layer of Al was deposited subsequently as the protecting layer. The current−voltage characteristics were measured using a Hewlett-Packard 4155B semiconductor parameter analyzer. The power of the EL emission was measured using a Newport 2835-C multifunction optical meter. The brightness was calculated using the forward output power and the EL spectra of the devices; a Lambertian distribution of the EL emission was assumed.

Results and Discussion

Figure 1 displays the ^{1}H NMR spectra of Cl-POSS, POSS-CH_3 (**1**), and POSS-CH_2Br (**2**). The CH_2 peak of Cl-POSS (4.47 ppm) shifted downfield to 5.14 ppm in POSS-CH_3. The ratio of the peak areas of the benzylic CH_2 and CH_2Br protons is ca. 1:2. Taken together, these data suggest that Cl-POSS had reacted with 2,5-dimethylphenol to form POSS-CH_3. Table 1 lists the thermal properties and molecular weight distributions of the POSS-PPV-*co*-MEHPPV copolymers. Both the thermal degradation and glass transition temperatures increased substantially as the amount of POSS in MEHPPV increased, particularly for the case where 10 mol % POSS was tethered to MEHPPV: we observed an 83 °C increase in the value of T_d and a disappearance of any glass transition.[21b] This situation arose because

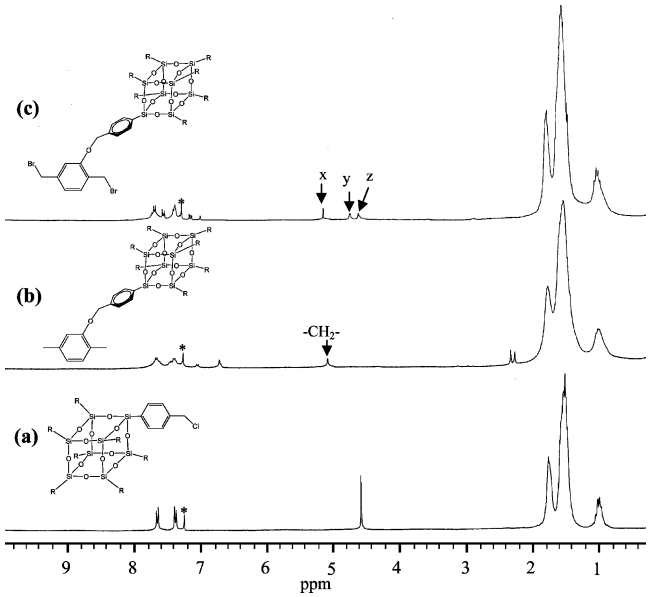

Figure 1. ^{1}H NMR spectra of (a) Cl-POSS, (b) POSS-CH_3, and (c) POSS-CH_2Br.

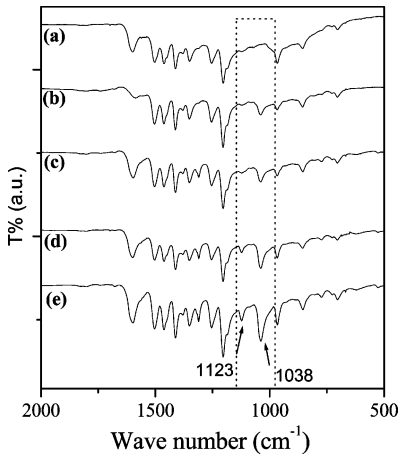

Figure 2. FTIR spectra of (a) MEHPPV, (b) POSS-PPV1-*co*-MEHPPV, (c) POSS-PPV3-*co*-MEHPPV, (d) POSS-PPV5-*co*-MEHPPV, and (e) POSS-PPV10-*co*-MEHPPV.

the tethered bulky POSS enhanced the thermal stability and retarded the mobility of the polymer main chain. The molecular weights of the POSS-PPV-*co*-MEHPPV copolymers decreased upon increasing the POSS content; this phenomenon can be attributed to the steric hindrance caused by the POSS units during the polymerization process. Figure 2 displays FTIR spectra of MEHPPV copolymers containing different amounts of POSS. The FTIR spectrum of POSS displays two major characteristic peaks: the Si−C band at 1038 cm^{-1} and the Si−O−Si band at 1123 cm^{-1}.

Table 2 lists the wavelengths of the absorption, the location of the PL maxima, and the quantum yields of POSS-PPV-*co*-MEHPPV. The absorption and emission

Table 2. Optical Properties of the POSS-PPV-*co*-MEHPPV Nanocomposites

	λ_{max} (UV, nm)		λ_{max} (PL, nm)[a]		QY
	solution[b]	film	solution[b]	film	film[c]
MEHPPV	499	517	553 (592)	591 (634)	0.19
POSS-PPV1-*co*-MEHPPV	499	512	552 (591)	588 (633)	0.43
POSS-PPV3-*co*-MEHPPV	498	512	552 (591)	586 (632)	0.62
POSS-PPV5-*co*-MEHPPV	497	511	552 (591)	585 (631)	0.84
POSS-PPV10-*co*-MEHPPV	494	505	551 (590)	584 (631)	0.87

[a] The data in parentheses are the wavelengths of the shoulders and subpeaks. [b] The absorption and emission were measured in THF. [c] PL quantum yield estimated relative to a sample of Rhodamine 6G ($\Phi_r = 0.95$).[23−25]

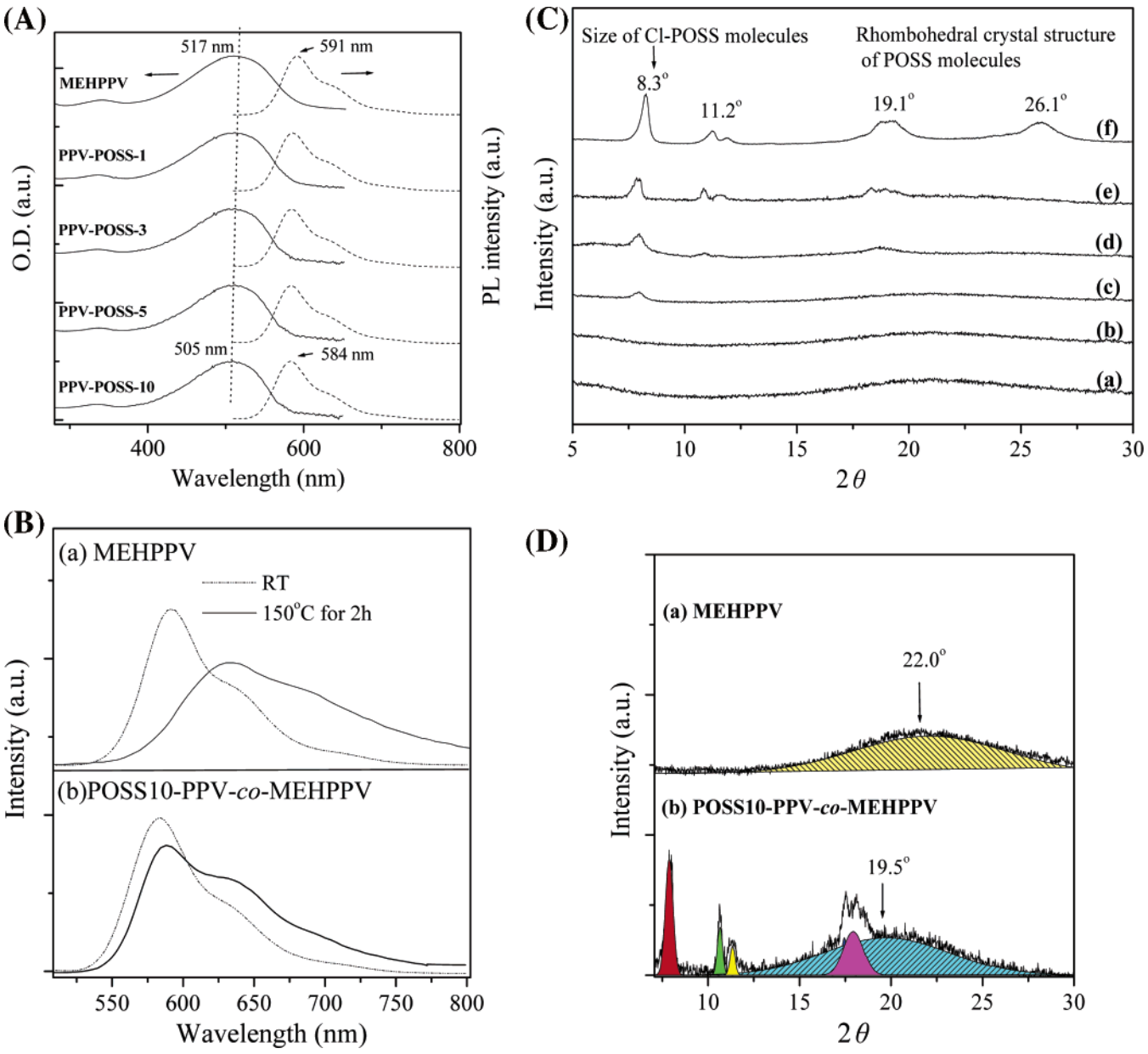

Figure 3. (A) UV−vis absorption and PL spectra of (a) MEHPPV, (b) POSS-PPV1-*co*-MEHPPV, (c) POSS-PPV3-*co*-MEHPPV, (d) POSS-PPV5-*co*-MEHPPV, and (e) POSS-PPV10-*co*-MEHPPV recorded in the solid state. (B) Normalized (relative to their maximum wavelengths) PL spectra of (a) MEHPPV and (b) POSS-PPV10-*co*-MEHPPV annealed at room temperature and 150 °C in the solid state. (C) X-ray diffraction spectra of (a) MEHPPV, (b) POSS-PPV1-*co*-MEHPPV, (c) POSS-PPV3-*co*-MEHPPV, (d) POSS-PPV5-*co*-MEHPPV, (e) POSS-PPV10-*co*-MEHPPV, and (f) Cl-POSS. (D) Deconvoluted X-ray diffraction spectra of (a) MEHPPV and (b) POSS-PPV10-*co*-MEHPPV.

peak maxima of MEHPPV occurred at 499 and 553 nm, respectively; these values are close to those reported in the literature.[19] We observed no aggregation band in these spectra because THF is a good solvent for MEH-PPV. The absorption and emission peaks for MEHPPV and POSS-PPV-*co*-MEHPPV are almost identical. For each polymer, the absorption peak maximum in solution (THF) is located between 499 and 494 nm, with a slight blue shift caused by the presence of POSS; the PL maxima occur at similar wavelengths for all of the polymers. Figure 3A presents the normalized absorption and PL emission spectra of the MEHPPV−POSS co-

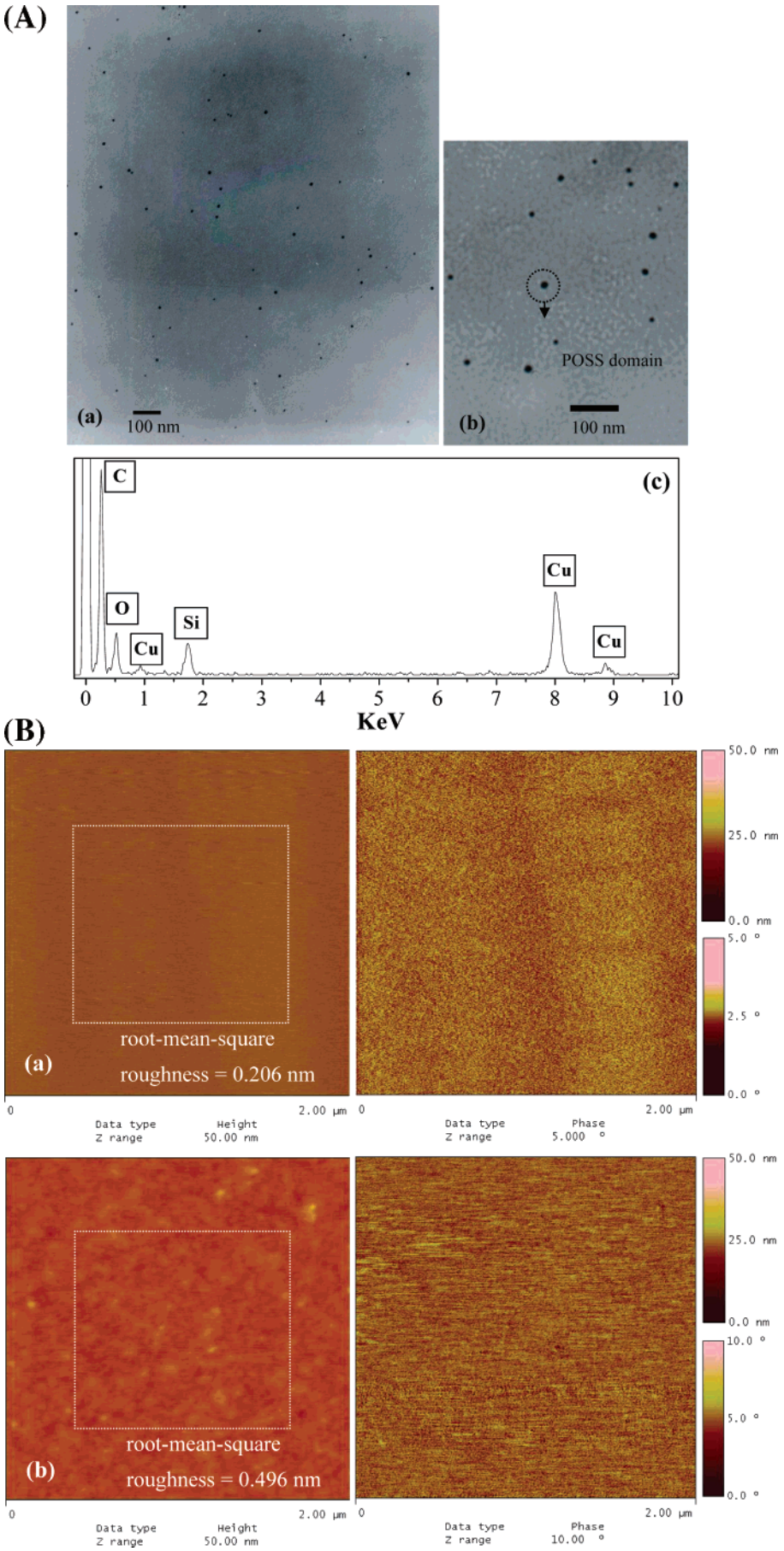

Figure 4. (A) (a) Transmission electron micrograph of POSS-PPV10-*co*-MEHPPV; (b) enlarged view; (c) EDS of POSS-PPV10-*co*-MEHPPV. (B) Surface roughness of thin films of (a) MEHPPV and (b) POSS-PPV10-*co*-MEHPPV.

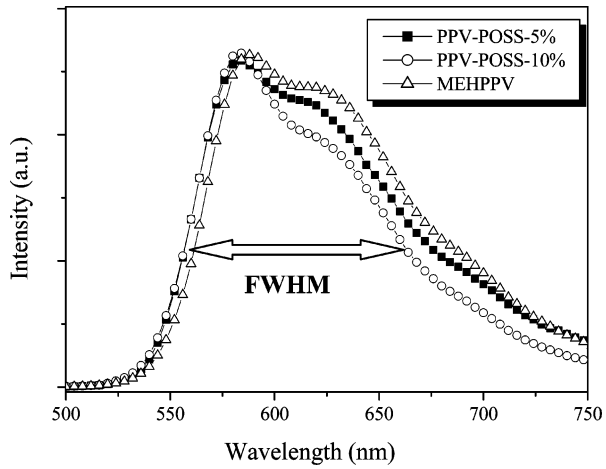

Figure 5. Electroluminescence spectra of the devices prepared from POSS-PPV-*co*-MEHPPV in the configuration ITO/PEDOT/polymer/Ca/Al.

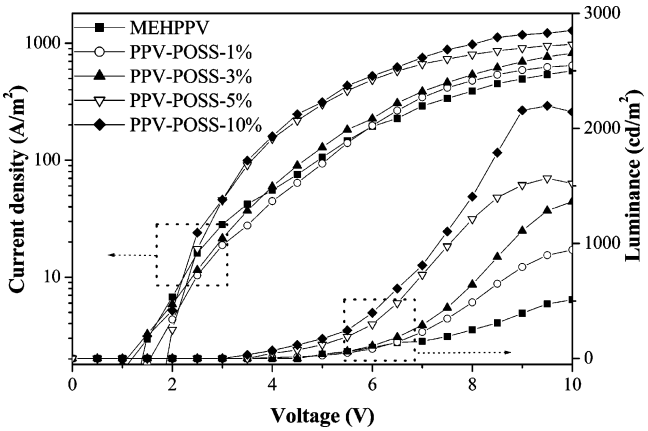

Figure 6. *I*−*L*−*V* curves of the devices prepared from POSS-PPV-*co*-MEHPPV and MEHPPV in the configuration ITO/PEDOT/polymer/Ca/Al.

polymer films. The quantum yields of the POSS-PPV-*co*-MEHPPV copolymers increased substantially as the amount of tethered POSS increased.[30] In particular, the quantum yield of MEHPPV containing 10% POSS was 4 times higher than that of pure MEHPPV (0.87 vs 0.19). We attribute this finding to the steric hindrance caused by the POSS units in preventing aggregation of the PPV main chains, which, in turn, reduces the degree of dimer formation after excitation. This improved quantum yield, which has not been reported in any previous studies of POSS/PPV copolymers, is a direct result of employing this particular side-chain-tethered POSS architecture.

For fresh MEH-PPV film, the yellowish peak at ~590 nm originates from single chain exciton emissions,[26] whereas the reddish peak at 630 nm is related to emissions from interchain species, such as aggregates or excimers.[26a] The difference in the PL spectra of the fresh MEH-PPV and POSSPPV-*co*-MEHPPV film is small because both polymer chains have not reached equilibrium states by their preparation process (i.e., spin-coating). By annealing the polymer films at higher temperatures as in the work by Schwartz[27] and Yang Yang[28] et al., one could see some more profound changes in their PL spectra. For instance, Figure 3B shows that after annealing MEHPPV film at 150 °C for 2 h under air its PL spectrum displays a red-shifted broad main peak at 630 nm, indicating formation of aggregates. While the main emission peak for annealed POSS-PPV10-*co*-MEHPPV film remain near 590 nm, with a weak peak at 630 nm. Therefore, at the equilibrium states, there is a distinct difference in their PL spectra, due to the bulky and rigid POSS groups tethered to the side of MEHPPV chains. The same phenomena are also observed in EL spectra (Figure 5).

We have carried out X-ray diffraction studies for confirming that interchain distance of PPV was increased by side-chain-tethered POSS. Figure 3C displays the X-ray diffraction curves of Cl-POSS, MEHPPV, and PPV-POSS. There are three distinct diffraction peaks at $2\theta = 8.3°$, 19.1°, and 26.1° for Cl-POSS (Figure 3f), which correspond to *d*-spacings of 10.5, 4.6, and 3.3 Å, respectively. The *d*-spacing of 10.5 Å reflects the size of the Cl-POSS molecules; the other two spacings are owing to the rhombohedral crystal structure of POSS molecules.[29a] For pure MEHPPV and PPV−POSS copolymers, it is evident that they are amorphous and have no side chain alignment. The nearly amorphous structure of pure MEHPPV (Figure 3C-a) originates from the two highly asymmetric substituents: the methoxy and 2-methoxy 5-(2′-ethoxyhexyloxy) for MEH-PPV.[29b] When POSS molecules were tethered to PPV, the average interchain distance increased appreciably from X-ray diffraction results. For instance, in the presence of 10% POSS (PPV-POSS-10%), the interchain distance increases to 4.6 Å (19.5°) from 4.0 Å (22.0°) for MEHPPV after deconvolution of the X-ray diffraction curve.

Figure 4A presents a transmission electron microscopy (TEM) image of our POSS-PPV10-*co*-MEHPPV sample.[31] This image reveals that no large aggregates were formed, but small domains of POSS are present; these POSS domains are dispersed evenly in the polymer matrix—a situation that we confirmed by analyzing this sample's energy dispersive spectrum (EDS; Figure 4A-c). The topology of POSS-PPV-*co*-MEHPPV copolymers films were studied with atomic force microscopy (AFM). Figure 4B shows the height image and the phase image of MEH-PPV and POSS-PPV10-*co*-MEHPPV polymer films prepared with chlorobenzene as the solvent. The surface roughness of PPV-POSS film is larger than that of pure MEHPPV (0.496 nm vs 0.206 nm) due to the presence of POSS. The phase images also show that POSS groups are dispersed homogeneously in the whole system.

Electroluminescence Characteristics. Figure 5 displays the electroluminescence (EL) spectra of POSS-PPV-*co*-MEHPPV devices. The EL device prepared from MEHPPV emits a strong peak at 590 nm and a vibronic signal in the range 610−620 nm, which is due presumably to the aggregation of MEHPPV and its excimer formation, as discussed earlier. The introduction of bulky siloxane units into the PPV side chains presumably increases the interchain distance, thereby retarding interchain interactions and leading to a reduction in the degree of exciton migration to defect sites.[22] Figure 6 displays the variations in the current density and brightness of the EL devices. The turn-on voltage decreased to 2.5 V for PPV containing 10% POSS from 3.5 V for the pure-MEHPPV EL device. As indicated in Figure 6, a more than 4-fold increase in the maximum brightness of the POSS-PPV10-*co*-MEHPPV device occurs with respect to that of the pure-MEHPPV EL device (2196 vs 473 cd/m^2) at a driving voltage of 9.5 V. The efficiency of POSS-PPV10-*co*-MEHPPV is 1.83 cd/A at a current density of 1221 A/m^2.

These improvements might be due to a decreased degree of aggregation upon the incorporation of the POSS units into the PPV chains.

Summary

We have synthesized a novel poly(*p*-phenylenevinylene) side-chain-tethered polyhedral silsesquioxane (POSS-PPV-*co*-MEHPPV) that possesses a well-defined architecture. This particular molecular architecture of PPV-POSS increases the quantum yield of MEHPPV significantly by reducing the degree of interchain aggregation; it also results in a much brighter red light from the EL device by decreasing the degree of aggregation between the polymer chains.

Acknowledgment. We acknowledge Chunghwa Picture Tubes, Ltd., and the National Science Council, Taiwan, for funding this work through Grant NSC 94-2120-M-009-001. Mr. Chen-Ping Chen and Mr. Yao-Te Chang are also acknowledged for experimental assistance and helpful discussions.

Supporting Information Available: Normalized UV–vis absorption and photoluminescence spectra and DSC and TGA traces of MEHPPV and PPV-POSS. This material is available free of charge via the Internet at http://pubs.acs.org.

References and Notes

(1) Ranger, M.; Rondeau, D.; Leclerc, M. *Macromolecules* **1997**, *30*, 7686.
(2) Yu, W.-L.; Pei, J.; Cao, Y.; Huang, W.; Heeger, A. J. *Chem. Commun.* **1999**, 1837.
(3) Pei, J.; Yu, W.-L.; Huang, W.; Heeger, A. J. *Chem. Commun.* **2000**, 1631.
(4) Ego, C.; Marsitzky, D.; Becker, S.; Zhang, J.; Grimsdale, A. C.; Müllen, K.; MacKenzie, J. D.; Silva, C.; Friend, R. H. *J. Am. Chem. Soc.* **2003**, *125*, 437.
(5) Mitschke, U.; Baüerle, P. *J. Mater. Chem.* **2000**, *10*, 1471.
(6) Kraft, A.; Grimsdale, C.; Holmes, A. B. *Angew. Chem., Int. Ed.* **1998**, *37*, 402.
(7) (a) Sokolik, I.; Yang, Z.; Karasz, F. E.; Morton, D. C. *J. Appl. Phys.* **1993**, *74*, 3584. (b) Hsieh, B. R.; Yu, Y.; Forsythe, E. W.; Schaaf, G. M.; Feld, W. A. *J. Am. Chem. Soc.* **1998**, 231. (c) Johansson, D. M.; Srdanov, G.; Yu, G.; Theander, M.; Inganas, O.; Andersson, M. R. *Macromolecules* **2000**, *33*, 2525.
(8) (a) Yang, Z.; Karasz, F. E.; Geise, H. J. *Macromolecules* **1993**, *26*, 6570. (b) Spreitzer, H.; Becker, H.; Kluge, E.; Kreuder, W.; Schenk, H.; Demandt, R.; Schoo, H. *Adv. Mater.* **1998**, *10*, 1340. (c) Ahn, T.; Jang, M. S.; Shim, H.-K.; Hwang, D.-H.; Zyung, T. *Macromolecules* **1999**, *32*, 3279. (d) Becker, H.; Spreitzer, H.; Ibrom, K.; Kreuder, W. *Macromolecules* **1999**, *32*, 4925. (e) Becker, H.; Spreitzer, H.; Kreuder, W.; Kluge, E.; Schenk, H.; Parker, I.; Cao, Y. *Adv. Mater.* **2000**, *12*, 42.
(9) (a) Pasco, S. T.; Lahti, P. M.; Karasz, F. E. *Macromolecules* **1999**, *32*, 6933. (b) Chen, Z. K.; Lee, N. H. S.; Wei, H.; Xu, Y. S.; Cao, Y. *Macromolecules* **2003**, *36*, 1009.
(10) Jin, S. H.; Jung, J. E.; Park, D. K.; Jeon, B. C.; Kwon, S. K.; Kim, Y. H.; Moon, D. K.; Gal, Y. S. *Eur. Polym. J.* **2001**, *37*, 921.
(11) Lee, S. H.; Jin, S. H.; Moon, S. B.; Song, I. S.; Kim, W. H.; Kwon, S. K.; Park, N. K.; Han, E. M. *Mol. Cryst. Liq. Cryst.* **2000**, *349*, 507.
(12) (a) Jin, S. H.; Kim, W. H.; Song, I. S.; Kwon, S. K.; Lee, K. S.; Han, E. M. *Thin Solid Films* **2000**, *363*, 255. (b) Huber, J.; Mullen, K.; Salbeck, J.; Schenk, H.; Scherf, U.; Stehlin, T.; Stern, R. *Acta Polym.* **1994**, *45*, 244. (c) Lemmer, U.; Heun, S.; Mahrt, R. F.; Scherf, U.; Hopmeier, M.; Sieger, U.; Gobel, E. O.; Mullen, K.; Bassler, H. *Chem. Phys. Lett.* **1995**, *240*, 373. (d) Grell, M.; Bradley, D. D. C.; Ungar, G.; Hill, J.; Whitehead, K. S. *Macromolecules* **1999**, *32*, 5810.
(13) (a) Xiao, S.; Nguyen, M.; Gong, X.; Cao, Y.; Wu, H.; Moses, D.; Heeger, A. J. *Adv. Funct. Mater.* **2003**, *13*, 25. (b) Lin, W. J.; Chen, W. C.; Wu, W. C.; Niu, Y. H.; Jen, A. K. Y. *Macromolecules* **2004**, *37*, 2335. (c) Lee, J.; Cho, H.-J.; Jung, B.-J.; Cho, N. S.; Shim, H.-K. *Macromolecules* **2004**, *37*, 8523.
(14) Kulkarni, A. P.; Jenekhe, S. A. *Macromolecules* **2003**, *36*, 5285.
(15) Zhang, C.; Babonneau, F.; Bonhomme, C.; Laine, R. M.; Soles, C. L.; Hristov, H. A.; Yee, A. F. *J. Am. Chem. Soc.* **1998**, *120*, 8380.
(16) Lichtenhan, J. D.; Vu, N. Q.; Carter, J. A.; Gilman, J. W.; Feher, F. J. *Macromolecules* **1993**, *26*, 2141.
(17) Lichtenhan, J. D.; Otonari, Y. A.; Carr, M. J. *Macromlecules* **1995**, *28*, 8435.
(18) Feher, F. J.; Soulivong, D.; Eklud, A. G.; Wyndham, K. D. *Chem. Commun.* **1997**, 1185.
(19) (a) Gustafsson, G.; Cao, Y.; Treacy, G. M.; Klavetter, F.; Colaneri, N.; Heeger, A. J. *Nature (London)* **1992**, *357*, 477. (b) Aratani, S.; Zhang, C.; Pakbaz, K.; Hoger, S.; Wudl, F.; Heeger, A. J. *J. Electron. Mater.* **1993**, *22*, 745. (c) Yang, Y.; Heeger, A. J. *Appl. Phys. Lett.* **1994**, *64*, 1245. (d) Braun, D.; Heeger, A. J. *Appl. Phys. Lett.* **1991**, *58*, 1982.
(20) (a) Leu, C. M.; Reddy, G. M.; Wei, K. H.; Shu, C. F. *Chem. Mater.* **2003**, *15*, 2261. (b) Leu, C. M.; Chang, Y. T.; Wei, K. H. *Chem. Mater.* **2003**, *15*, 3721. (c) Leu, C. M.; Chang, Y. T.; Wei, K. H. *Macromolecules* **2003**, *36*, 9122.
(21) (a) Chou, C.-H.; Hsu, S.-L.; Dinakaran, K.; Chiu, M.-Y.; Wei, K.-H. *Macromolecules* **2005**, *38*, 745. (b) Chen, S. H.; Su, A. C.; Chou, H. L.; Peng, K. Y.; Chen, S. A. *Macromolecules* **2004**, *37*, 167.
(22) Grimsdale, A. C.; Leclère, P.; Lazzaroni, R.; MacKenzie, J. D.; Murphy, C.; Setayesh, S.; Silva, C.; Friend, R. H.; Müllen, K. *Adv. Funct. Mater.* **2002**, *12*, 729.
(23) Kurian, A.; George, N. A.; Paul, B.; Nampoori, V. P. N.; Vallabhan, C. P. G. *Laser Chem.* **2002**, *20*, 99.
(24) Heldt, J. R.; Heldt, J.; Obarowska, M.; Mielewska, B.; Kamiński, J. *J. Fluoresc.* **2002**, *11*, 335.
(25) Magde, D.; Wong, R.; Seybold, P. G. *Photochem. Photobiol.* **2002**, *75*, 327.
(26) (a) Shi, Y.; Liu, J.; Yang, Y. *J. Appl. Phys.* **2000**, *87*, 4254. (b) Nguyen, T.-Q.; Martini, I.; Liu, J.; Schwartz, B. J. *J. Phys. Chem. B* **2000**, *104*, 237. (c) Nguyen, T.-Q.; Doan, V.; Schwartz, B. J. *J. Chem. Phys.* **1999**, *110*, 4068.
(27) (a) Nguyen, T.-Q.; Schwartz, B. J.; Schaller, R. D.; Johnson, J. C.; Lee, L. F.; Haber, L. H.; Saykally, R. J. *J. Phys. Chem. B* **2001**, *105*, 5153. (b) Nguyen, T.-Q.; Schwartz, B. J. *J. Chem. Phys.* **2002**, *116*, 8198.
(28) (a) Liu, J.; Shi, Y.; Yang, Y. *Adv. Funct. Mater.* **2001**, *11*, 420. (b) Shi, Y.; Liu, J.; Yang, Y. *J. Appl. Phys.* **2000**, *87*, 4254.
(29) (a) Zheng, L.; Waddon, A. J.; Farris, R. J.; Coughlin, E. B. *Macromolecules* **2002**, *35*, 2375. (b) Tretiak, S.; Saxena, A.; Martin, R. L.; Bishop, A. R. *J. Phys. Chem. B* **2000**, *104*, 7029.
(30) (a) PL quantum yield (Φ_{FL}) was determined by using Rhodamine 6G ($\Phi_r = 0.95$) as a reference that is dispersed in poly(methyl methacrylate) (PMMA) at low concentration (10^{-3} M) with the film thickness being 100 ± 10 nm. The quantum yield of a sample, Φ_s, can be calculated by the following equation: $\Phi_s = (A_r/A_s)(F_s/F_r)\Phi_r$, where A_s and A_r are the respective optical density of the sample and the reference at their excitation wavelengths and F_r and F_s are the corresponding areas under their emission peaks. (b) Kang, B. S.; Kim, D. H.; Lim, S. M.; Kim, J.; Seo, M.-L.; Bark, K.-M.; Shin, S. C.; Nahm, K. *Macromolecules* **1997**, *30*, 7196.
(31) Transmission electron microscopy was performed on a Hitachi H-600 instrument operated at 100 kV and on a JEOL-2010 TEM operated at 200 kV at the Center for Nano Science & Technology (CNST). The ultrathin sections of POSS-PPV-*co*-MEHPPV copolymer prepared for TEM studies were microtomed using a Leica Ultracut Uct apparatus equipped with a diamond knife and subsequently deposited on copper grids. The microtomed thin films, corresponding to the section of the POSS-PPV-*co*-MEHPPV copolymer, were also observed using a Digital Nanoscope IIIa atomic force microscope (AFM).

MA051055U